FIELD INVESTIGATION OF CO_2 UPTAKE IN SITKA SPRUCE

by

JEREMY. H. GRIFFITHS

A thesis submitted in fulfilment of the requirement

for the degree Master of Philosophy

to the

University of Edinburgh

1983

ABSTRACT

A portable gas exchange system was developed which enabled net photosynthesis, respiration and stomatal conductance to be measured on conifers. The technique was developed using principles employed in the null-balance diffusion porometer. The system was particularly suited to field conditions where there is no external power supply. Measurements could be made on a large number of different shoots or repeatedly on the same shoot. Up to 150 measurements could be made within a day by two people.

The equipment was thoroughly tested in the laboratory before field use. Particular attention was paid to the infra-red gas analyser which was a new instrument that had not been previously tested in the field. Functional tests were carried out on the system as a whole to assess its suitability as a field instrument. Problems normally associated with diffusion porometers such as the changing leaf and chamber temperature were investigated.

The system was used to investigate the distribution of photosynthesis within the canopy of a Sitka spruce forest. Measurements were made over a number of months on various components of the canopy. Terminal and lateral shoots from different whorls and of different ages were investigated. Non-linear regression techniques were used to fit a non-rectangular hyperbolic function to the data in an attempt to account for the effects of variables such as quantum flux density and stomatal conductance. The function provided an adequate description of the data in terms of biologically meaningfull parameters such as the quantum efficiency and mesophyll resistance to CO_2. The parameters were subsequently used to predict rates of net

photosynthesis of different levels of foliage in response to quantum flux density.

The results showed that the photosynthetic potentials of shoots on different whorls above the level of canopy closure were not very different. The major differences were between shoots above and below this level. Current year shoots consistently had higher photosynthetic potentials than one-year-old shoots.

The fieldwork showed that the technique was suitable for this type of study and that it had several advantages over previous methods.

DECLARATION

This thesis has been composed by myself and it has not been submitted in any previous application for a degree. The work reported within was executed by myself unless otherwise stated.

ACKNOWLEDGEMENTS

I would like to express my sincere gratitude to my supervisor, Professor P. G. Jarvis for his guidance and encouragement throughout this work.

I am grateful to the Institute of Terrestrial Ecology for the use of the experimental site and facilities at Rivox. In particular I would like to thank Dr. E. D. Ford for acting as a supervisor whilst Professor Jarvis was in Australia.

I would also like to thank Mr. Andrew Sanford for his advice and practical help with electronics and computing.

Finally I would like to thank all those who spared the time to help me in the field for their hard work and patience.

CONTENTS

CHAPTER 1

INTRODUCTION

1.1 Preface

The first objective of this project was to develop a quick, simple, portable technique for measuring photosynthesis in the field extensively. The aim was to fill the gap existing between assimilation chamber and $14-CO_2$ techniques. The concept of a CO_2 porometer was to be put into practice and thoroughly tested in the laboratory and field.

The second objective of the work involved an extensive investigation of the distribution of photosynthesis within a forest canopy, for which the equipment was particularly suited. The Sitka spruce (*Picea sitchensis* Bong. Carr) canopy to be studied had previously been investigated with respect to stomatal conductance (Leverenz *et al*, 1982). It was hoped that a study of the spatial distribution of photosynthesis would lead to a proper description of the source and size of variation to assess the role of canopy structure on photosynthesis.

1.2 Gas exchange studies

Gas exchange studies on plants have successfully been carried out over the past 25 years utilising mobile laboratories. Such systems are usually costly and limited in their use because the instruments are not truly portable. A gas exchange system for carbon dioxide and water vapour that can be conveniently carried and operated by one or two people would have a distinct advantage. Several portable systems have been designed and tested using radioactive isotopes (e.g. Bravdo 1972; Johnson, Rowlands, and Ting 1979) but these have the disadvantages associated with radioactive techniques.

A more suitable instrument for carbon dioxide analysis is the infrared gas analyser (IRGA) (Sestak, Catsky and Jarvis 1971). However the majority of IRGA's are designed for industrial or laboratory use and are not particuarly suited for operation in the field. Nearly all IRGA's require a stable, constant frequency, a.c. supply to ensure steady operation of fluctuation-sensitive components such as mechanical choppers. Such requirements call for considerable precautions when operating IRGA's under field conditions (Sestak et al 1971). IRGA's in the field are normally mounted in such a way as to avoid vibration, usually in mobile laboratories that are maintained at constant temperature by air conditioning equipment (Mooney et al 1971). A power supply from the electrical grid is desirable, since a.c generators are generally not free from voltage and frequency fluctuations. Alternatively voltage stabilizers with frequency compensation may be used in conjunction with the generator, or a d.c./a.c. converter powered by batteries. However many IRGA's are internally thermostated and draw too much current for regular supply from batteries.

IRGA's have most widely been used in the field for intensive measurements on a few leaves. Occasionally they have been built into gas switching systems which have enabled twenty or more samples to be measured sequentially (e.g. Sinclair et al 1979; Troeng and Linder 1981) but in general they have not been used for extensive measurements of the rates of photosynthesis of large numbers of leaves. However, for many purposes it is desirable to be able to make spot measurements on a large number of samples to estimate the rate of photosynthesis by different plants, parts of canopies and entire canopies. In the recent past $14-CO_2$ methods have been used for this purpose (e.g. Shimshi 1969; Nielson 1978; Bell 1981) but these methods suffer from several disadvantages: they are not accurate; they require precautions in the use of the isotope; they require as much time spent in the laboratory as the field; the digestion and scintillation cocktails are expensive; special precautions must be taken to avoid loss of activity between feeding and analysis; and respiration cannot be measured. Recently, three methods have been described for the collection of small gas samples from porometer chambers in the field and their subsequent analysis by IRGA in the laboratory (e.g. Fanjul, Jones and Treharne 1980; Parkinson, Day and Leach 1980; Ehleringer and Cook 1980). These methods involve careful handling of the gas samples in the field and calibration of the IRGA to obtain accurate measurement from the passage of a pulse of sample gas in a carrier and require a considerable amount of additional time to be spent in the laboratory. For these reasons, a CO_2 porometer using a portable IRGA in the field would have considerable advantages.

1.3 Theory

The basic concept of the CO_2 porometer is to add CO_2-enriched air to a chamber enclosing the leaves, at a rate sufficient to replace the CO_2 removed in photosynthesis. The CO_2 concentration inside the chamber is maintained at the ambient concentration (or any other specified concentration), the rate of net photosynthesis being obtained from the rate of inflow of CO_2-enriched air as described by Koller and Samish (1964). The operating system is essentially similar to that used with the null-balance diffusion porometer (Beardsell, Jarvis and Davidson 1972). A differential IRGA (Binos 2, Leybold Heraeus. See appendix 2), with ambient air as the flowing reference and air from the assimilation chamber in a closed loop with the sample cell, indicates departure from the null condition. A cylinder of compressed dry air, as used with the null-balance H_2O porometer, contains dry air enriched with CO_2. The rate of flow of this air into the assimilation chamber is measured with the same flow meter in two seperate measurements: one for the H_2O null-balance and one for the CO_2 null-balance. The absolute Binos is used continuously to monitor the CO_2 concentration of the ambient air and to balance at CO_2 concentrations other than ambient.

Consider leaves photosynthesising in a stirred assimilation chamber. If the CO_2 concentration in the chamber is kept constant by the addition of CO_2-enriched air to the chamber, the rate of photosynthesis by the leaves is equal to the net rate of addition of CO_2 to the chamber. Thus

$$F_b = f_b * z(C_c - C_b)/A \qquad (1.1)$$

where:

C_c is the concentration of CO_2 in the air being added from the cylinder (μmol mol^{-1}).

C_b is the concentration of CO_2 in the chamber at the balance point and is also the CO_2 concentration of the air leaving the chamber (normally equal to the ambient concentration) (μmol mol^{-1}).

f_b is the measured rate of inflow of air to the assimilation chamber (m^3 s^{-1}).

z is the density of CO_2 in air (mol m-3).

A is the leaf area (m^2), and

F_b is the rate of net photosynthesis at C_b (μmol m^{-2} s^{-1}).

A suitable CO_2 concentration of the balancing gas can be derived from the arrangement of equation (1.1) as follows:

$$C_c - C_b = F_b*A/(f_b*z) \qquad (1.2)$$

Thus if the maximum likely CO_2 flux is 20 μmol m^{-2} s^{-1} by a maximum enclosed leaf area of 30 cm^2, and the maximum flow rate possible is 30 cm^3 s^{-1}, the CO_2 concentration of the balancing gas needs to be at least 50 μmol mol^{-1} above the ambient CO_2 concentration. Balancing at high CO_2 fluxes is achieved more easily if the difference in concentration is about twice this value, although this may lead to some loss of sensitivity at low CO_2 fluxes. Since the ambient CO_2 concentration can also vary diurnally by as much as 50 μmol mol^{-1}, or more in growth rooms and glasshouses, a suitable general purpose balancing concentration is 450-500 μmol mol^{-1}.

Dark respiration can also be measured either by balancing at the ambient CO_2 concentration with CO_2-depleted air, or by balancing at a higher CO_2 concentration, say 600 μmol mol^{-1}, with the normal balancing gas.

CHAPTER 2

MATERIALS AND METHODS

2.1 Equipment

The Binos was not primarily designed as a field instrument, but has several important features which make it particularly suitable for field use. Compared to most other IRGA's, the Binos is very compact and light-weight because of its miniaturised components and C-MOS electronics. A standard half rack mounting (213x129x367 mm) can accommodate two separate sealed optical benches for the analysis of two different gases or simultaneous differential and absolute analysis of one, and weighs as little as 6.5 kg. The manufacturer's specifications suggest that the Binos is not influenced by vibration or position and that it may be used under field conditions where no secure mounting is available. The Binos is designed to operate at ambient temperatures from 0-45 C, with a typical influence of temperature of less than +0.1 % of range per K. The field instrument is not thermostatted, but the slow build up of temperature of the measuring cells is compensated for electronically. The stated warm-up time is 3 minutes, whereas most conventional IRGA's require several hours to reach a steady state. The Binos may be operated from a.c. mains voltage or from an 11-35 V d.c. supply. The power consumption for a two channel instrument with three small d.c. pumps (Brey G12/02) and liquid crystal displays is 19 VA.

The version of the Binos that was used in the gas exchange system, was a two channel instrument with absolute and differential gas paths and optics for measuring CO_2. The absolute channel had a sealed reference and measuring range of 0-500 μmol mol^{-1}; the differential

had a flowing reference gas path and a measuring range of ± 50 μmol mol^{-1}. Both channels had optical filters fitted to reduce the cross-sensitivity between CO_2 and H_2O. The output signals of both channels were linearised over their respective measuring ranges, although the differential channel output was said to be non-linear over the range 0 to -50 μmol mol^{-1}. The response time was initially set to 10 seconds, but is readily changed, and was adjusted to be 2 seconds.

The Binos was supplied in a full rack mounting (420x130x367 mm) to accommodate large facia mounted dust filters for each gas path, although the instrument itself only occupied half the available space. A number of modifications had to be made to the Binos to make it more suitable as a field instrument. The full rack case was replaced with a more secure custom built case measuring 245x290x380 mm. The gas path connections, along with the electrical sockets and fuses, were originally situated at the rear of the instrument where they could have easily become fouled if used in the field. These connections were repositioned at the front of the instrument, leaving the mains socket and fuse at the rear, protected by a cover. The gas path connections as supplied were not suitable for easy use in the field and were replaced with self-sealing connectors (Swagelok quick-fit SS-QC4-D-400) which allowed quick connection and protection of the gas paths from contamination. The internal plumbing of the Binos originally utilised rigid teflon tubing which was subsequently replaced with Viton tubing. Also the original common outlet was replaced with a separate outlet for each gas path to facilitate operation of the absolute and differential channels either in series or parallel. The facia mounted dust filters were exchanged for small inline filters (Whatman Mini Filter Grade inside the instrument case,

leaving room on the front panel for a separate pump switch and flowmeter (Rotameter 1300-2G-3101) for each of the three gas paths (one absolute gas path and two differential gas paths).

Other modifications included control circuits to enable the speed of the pumps to be varied and to allow the pumps to be switched together remotely.

The Binos was used in conjunction with a developed version of the null-balance H_2O porometer originally described by Beardsell *et al* (1972), built in 1977 by Dingbat Electronics, Aberdeen. Only minor modifications were necessary to use the two instruments together, but alterations were made to the chamber initially and at a later stage. The initial modifications involved replacing the top of the chamber with glass to allow better light transmission, and the addition of outlet and inlet ports to the chamber to accept air lines to and from the Binos.

The original chamber measured 90x75x70mm internally and was constructed of cross-linked polystyrene (Polypenco, Q 200.5) in two halves with silicon rubber seals on the abutting surfaces to form a good seal (Fig. 2.1). Below the main volume of the chamber there was a small perspex block housing a small fan along with a platinum resistance thermometer (PRT), and a Vaisala humidity sensor. Air was drawn from the chamber over the PRT and Vaisala sensor (Humicap 6061-HM) before returning to the chamber. The small fan caused mixing of air in the chamber to ensure uniform conditions throughout and also reduced the boundary layer resistance of any leaves that may be introduced. A quantum sensor (Li-Cor LI-190SB) for measuring photosynthetically active radiation (PAR) was attached to the outside of the chamber.

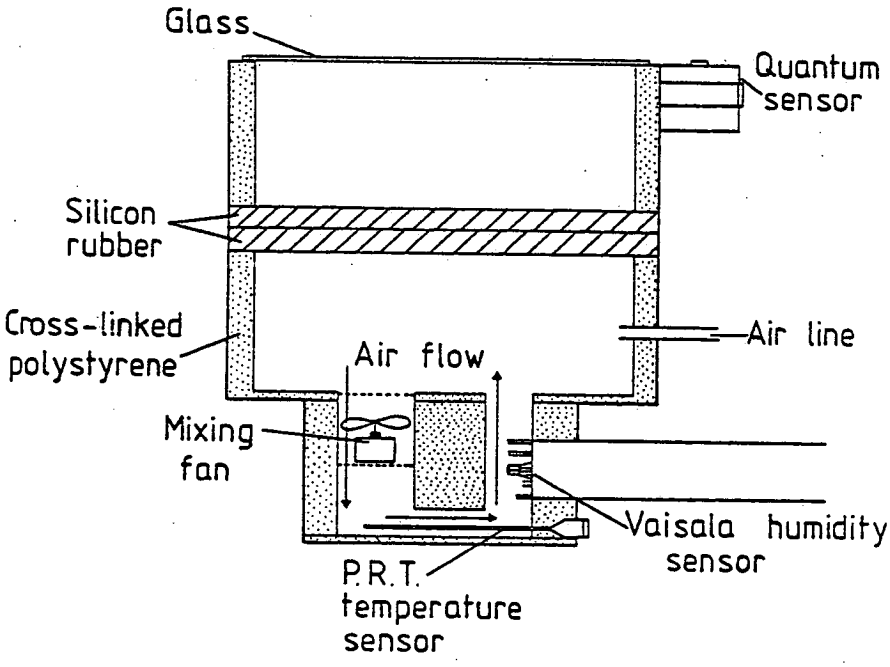

Fig. 2.1. A diagram of the original porometer chamber in cross-section.

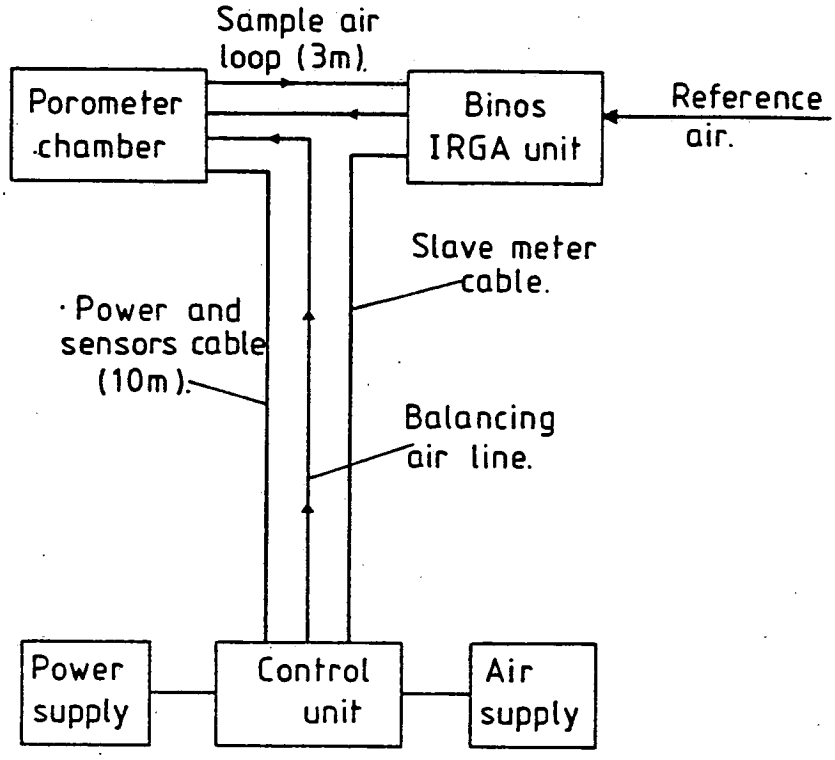

Fig. 2.2. A block diagram of the major components of the combined CO_2 and water vapour porometer.

The chamber was connected to the Binos differential sample channel in a closed loop by two polypropylene tubes (3 mm internal diameter, 3 m long). CO_2-enriched air was supplied to the chamber from a small aluminium cylinder via a needle valve in the control unit, through 10 m of 5 mm internal diameter PVC tubing (Fig. 2.2). Before the CO_2-enriched air entered the chamber it was passed through a drying tube containing silica gel, to ensure that the air was completely free from water vapour. The control unit was connected to the chamber sensors via a 12-core, shielded cable that also carried power to the chamber, from the control unit. A slave liquid crystal display and pump control switch, were connected to the Binos by a shielded 4-core cable, along with two 20 A cables to supply the Binos from a 12 V power source. The cable and tubing were all about 10 m in length, enabling a number of shoots to be sampled with the chamber without moving the control unit.

Later modifications included replacing the original PRT sensor with two semi-conductor temperature transducers (Farnell AD-590) that were considered more stable under field conditions. Both sensors were embeded in teflon rod, one being positioned inside the chamber below the fan, and the other below the chamber handle and protected from direct radiation. The control unit was modified so that either temperature sensor could be monitored. The needle valve controlling the chamber air supply was also exchanged for a more sensitive unit with a maximum flow rate of 15 cm^{-3} s- 1. A shut-off toggle valve was placed in the air supply line to allow the chamber air supply to be stopped quickly and to protect the needle valve by removing the need to shut off the air supply with the valve.

2.2 Operation

Stomatal conductance and CO_2 flux were measured sequentially on the same leaf or shoot. In most cases it was preferable to balance for humidity first to avoid any effects of low humidity on the stomata.

At the beginning of a set of measurements, the air lines, and in particular the drying tube containing silica gel, were flushed through with the balancing gas for a number of minutes to ensure the whole system came to equilibrium with respect to CO_2 concentration. The first measurement to be taken was the relative humidity of the ambient air (unless balancing to a different relative humidity) by holding open the chamber away from the operator. The value was recorded and the humidity null-balance point set to a zero reading on the control unit display by means of a potentiometer. The chamber was then closed around the plant material to be investigated and, if transpiration occured, the relative humidity within the chamber increased. Dry air was then introduced into the chamber at such a rate as to return and maintain the relative humidity within the chamber constant at the set point. The set point was indicated by a null reading, any divergence from the set point being indicated by a +/- reading. The flow rate was then recorded along with quantum flux density and temperature inside and outside of the chamber.

To measure CO_2 flux, the Binos pumps were switched on so that air from the chamber was circulated through the differential sample cell, whilst ambient air was passed through the reference cell of the differential and sample cell of the absolute channel (Fig. 2.3). If photosynthesis occured, the CO_2 concentration within the chamber decreased and was detected as a negative reading of the Binos differential channel. CO_2-enriched air was then added to the chamber

at such a rate as to return and maintain the CO_2 concentration inside the chamber at ambient concentration (or any other desired balancing concentration). The flow rate was then recorded along with the ambient CO_2 concentration, and the temperature and quantum flux readings were checked for any change.

Both measurements could be completed in under three minutes, allowing up to 20 pairs of measurements to be made in an hour. The porometer was operated by two people, one moving the chamber around the foliage with the other person adjusting flow rates and recording data. The measurements could be repeated on the same plant material a number of times before the leaves were removed to measure leaf area. The eventual destruction of plant material can be avoided when working with flat leaves, by using a chamber that encloses a fixed area.

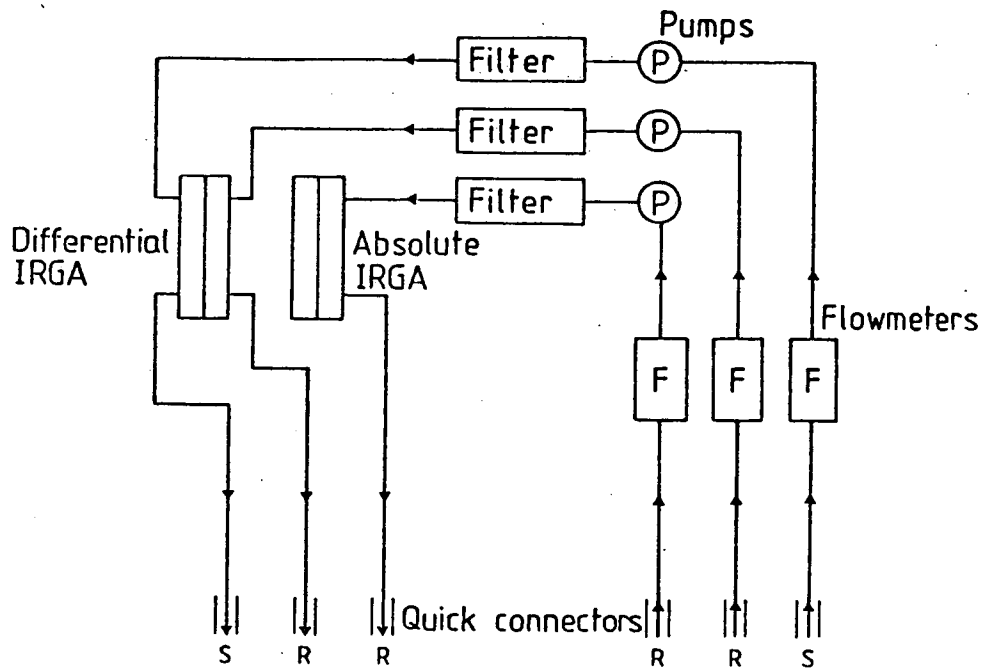

Fig. 2.3. A diagram of the flow paths of CO_2-enriched air through the Binos unit. S and R inicate the sample loop flow path and the reference air flow path respectively, in normal field use for the measurement of photosynthesis at ambient CO_2 concentration.

CHAPTER 3

TESTS AND CALIBRATIONS

Tests were carried out on the Binos to assess its suitability for use in a portable gas exchange system, with particular attention to its potential performance under field conditions.

3.1 Linearity

The Binos tested was supplied with a linearization option which the manufacturer's specifications suggest, should produce deviations of less than $\pm$ 1 %, over the measuring range. Linearization of the output signal is effected by seven potentiometers on the signal processing board which act independently at various points throughout the range. The non-linear signal voltages are slightly offset, so that they fall along the calculated linear plot of output against gas concentration. The effect of the linearization circuit may be seen by measuring the output voltages before and after linearization, over the measuring range (Fig. 3.1).

Linearity of either channel, can be easily adjusted using a millivoltmeter and a range of known CO_2 concentrations corresponding to the ranges of influence of the potentiometers. The response of the absolute channel was tested with CO_2 concentrations between 0 and 500 μmol mol^{-1}, produced by three gas- mixing pumps cascaded in series (Wosthoff type G27/3F, SA18/3F, SA27/3F). The concentrations measured with the Binos corresponded well with the calculated concentrations delivered by the gas-mixing pumps: the difference was never more than 2 μmol mol^{-1} ($\pm$0.4% of the measuring range), and some of this difference may be attributed to the mixing pumps which have been well

used over 5 years. Linearity of the differential channel was tested with air containing 330 μmol mol^{-1} CO_2 flowing through the reference side over a range of $\pm$ 50 μmol mol^{-1}. Fig. 3.2, shows that the output over this range may be considered linear, even though there was no provision for linearizing the negative signal over the range 0 to -50 μmol mol^{-1}.

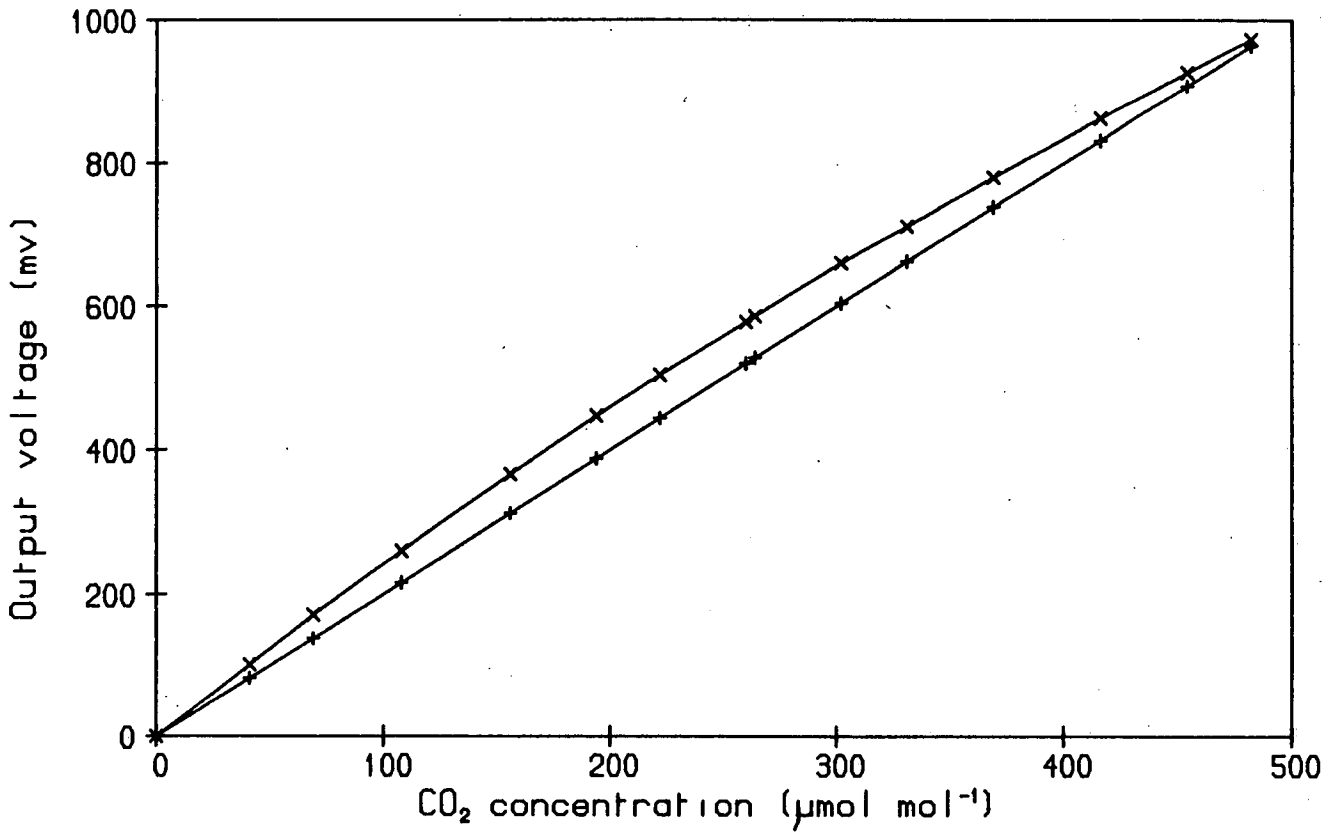

Fig. 3.1. Relationship between Binos output voltages and CO_2 concentrations supplied, before (—×—) and after (—+—) linearization, for the absolute channel.

3.2 Temperature influence and warm-up time

The zero point and sensitivity of both absolute and differential channels were carefully monitored during the first few weeks of use to assess their stability. The drifts of both zero and range were within the manufacturers specification of less than 2 % of measuring range per week for the zero point of either channel, and less than 0.3 % of measuring range per week for the sensitivity.

The influence of temperature, and the time required to reach the correct output value from switching on, were investigated under various ambient temperature conditions. When the Binos is first switched on, the zero of both channels steadily changes with time reaching steady, correct values after about 120 minutes at an ambient temperature of 20 ^{o}C (Fig. 3.3a), or 190 minutes at 6.5 ^{o}C. Copper-constantan thermocouples attached to the absolute and differential channels showed that zero was reached when the channel temperature reached about 40 ^{o}C, and the source temperature reached 60 ^{o}C. Although the Binos is temperature compensated to some extent there was a marked influence of temperature changes during the warm-up period on the output, but this effect was within the manufacturer's specification of less than + 0.1 % of range per ^{o}C. The stated warm-up time is two minutes, which is the time required for the measuring circuit to get in phase with the chopper. Controlled gas path heating and thermostatting up to 65 ^{o}C are both options, but neither would be practical for use in the field when operating from a battery. Experiments were carried out to heat up the source externally in an attempt to reduce the warm-up time. Heating coils consisting of 12 turns of 0.195 mm diameter, enamelled, copper/nickel (eureka or constantan) resistance wire, were placed around each channel at the

source end. Each heating coil had a resistance of 15 ohms and when supplied with 12 V d.c. from the battery supply, drew a current of 0.8 A. To achieve rapid warm-up, the heating coils are used when the Binos is first switched on, for a period of 5 to 15 minutes depending on the ambient temperature. This brings the temperature of the channels into the effective range of the compensation system, so that stable zero outputs are achieved after a further 15 minutes equilibration (Fig. 3.3b).

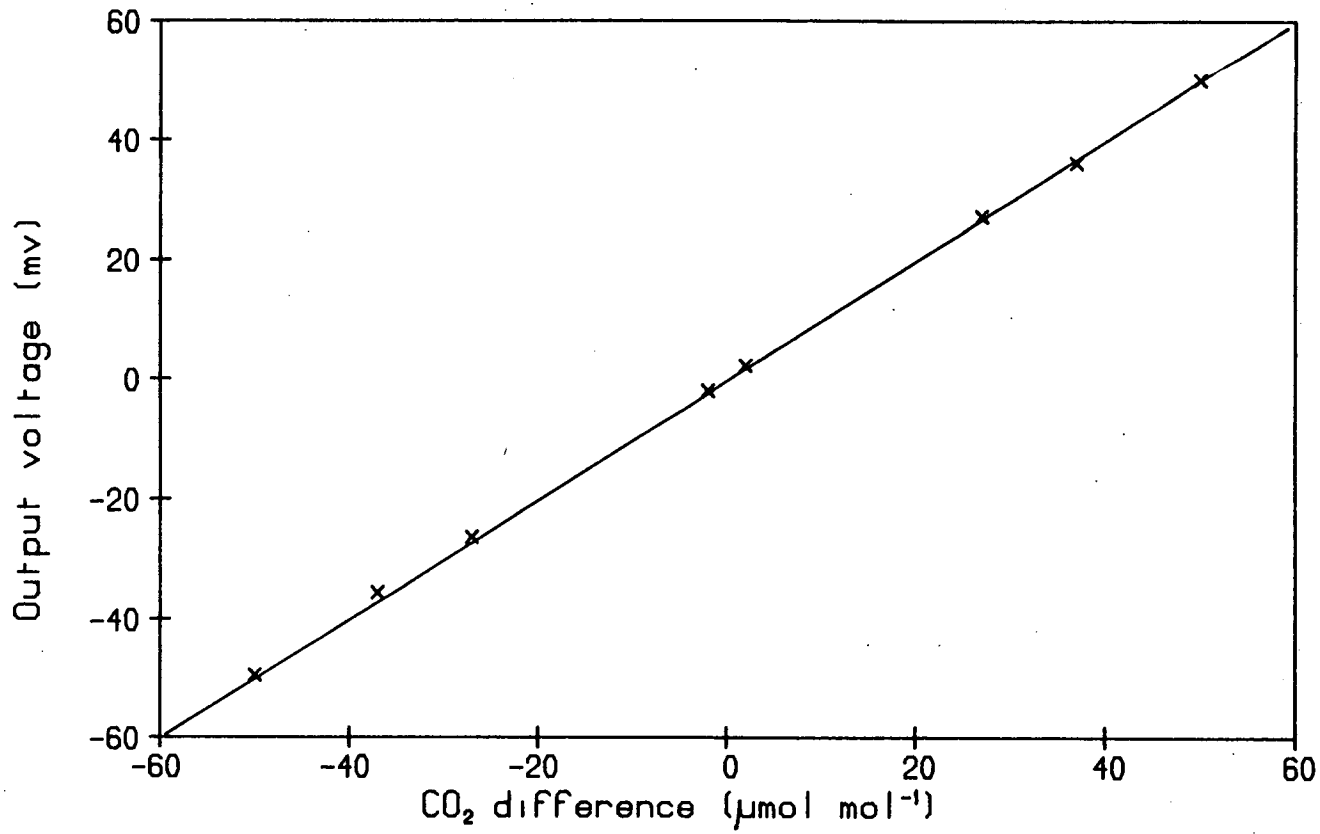

Fig. 3.2. Relationship between the Binos output voltages and the difference in CO_2 concentrations from 300 µmol mol^{-1} supplied, for the differential channel.

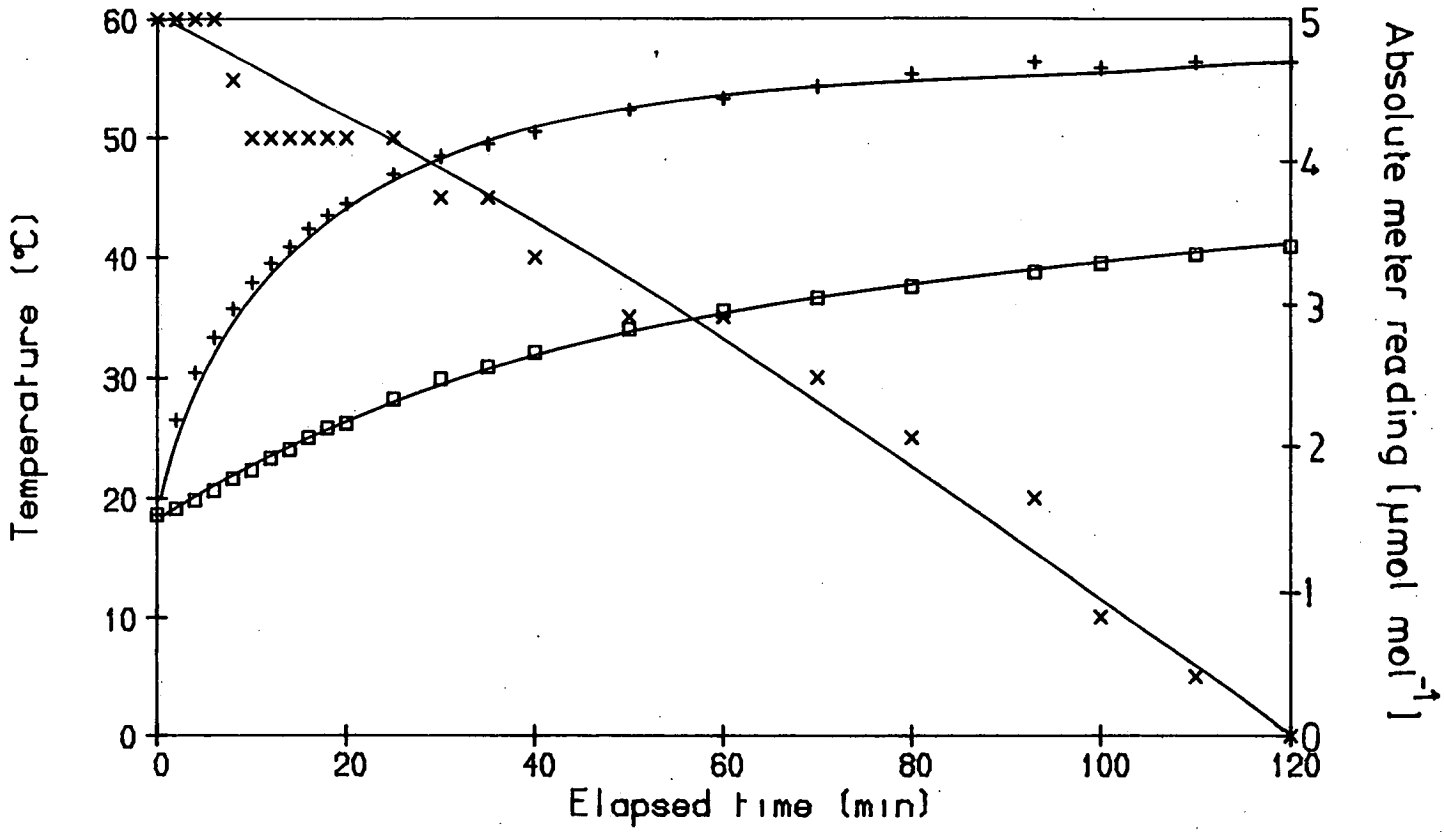

Fig. 3.3a. The warm up time of the Binos absolute channel without supplementary heating at 20 °C; (—+—) source temperature, (—□—) channel temperature, (—×—) meter reading, with CO_2-free air passing through the measuring cell.

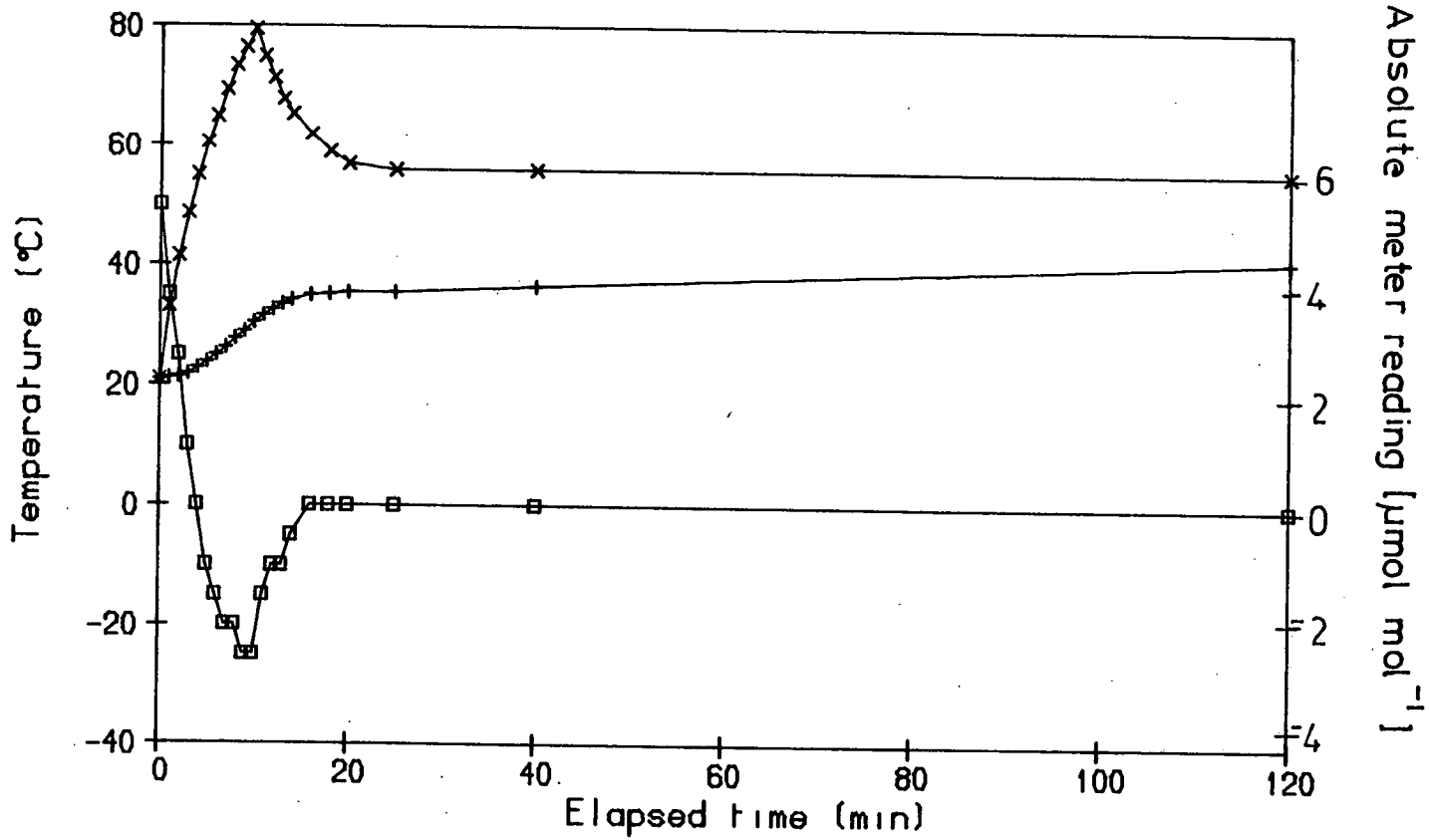

Fig. 3.3b. The warm up time of the Binos absolute channel with supplementary heating from copper/nickel heating coils; (—×—) source temperature, (—+—) channel temperature, (—□—) meter reading, with CO_2-free air passing through the measuring cell.

3.2 Pressure influences

Tests were also carried out to investigate the influence of air pressure on both channels. The absolute channel had a sealed reference cell and a sample cell that was vented to the atmosphere. The sample cell out-flow was blocked off and the cell air pressure varied by means of a pressure regulator and a cylinder of air of known volumetric CO_2 concentration. The internal cell pressure was measured with an electronic manometer referenced to known atmospheric air pressure. The output was recorded over a range of cell air pressures.

The differential channel had both reference and sample cells vented to the atmosphere. Pressure differences between the cells were set up as before and the effects recorded. The results showed the Binos to be within the manufacturers specification, with an influence of less than 0.1 % of range per 0.1 kPa difference in pressure between the cells.

Tests were also done with the differential sample cell connected to the porometer chamber in a closed loop to observe the effects of any resistance in the associated tubing. The results showed there to be negligible pressure difference between the sample and reference cells when operated in this manner.

3.4 Porometer tests

The null-balance diffusion porometer was calibrated before use in the following ways. The Vaisala humidity sensor was calibrated inside the chamber, using the water bath technique. Ambient air was first pumped through warmed water to saturate it with water vapour. The saturated air was then passed through coiled copper tubing immersed in a water bath of known temperature. The water bath was cooler than the the water used to saturate the air originally, which resulted in some

of the water vapour being condensed out to leave air saturated at the water bath temperature. The air was then passed into the chamber near the Vaisala sensor and the chamber air temperature monitored accurately. Knowing the water bath temperature and the chamber air temperature it was possible to calculate the relative humidity (RH) inside the chamber. The Vaisala was calibrated over a range of relative humidities achieved by altering the temperature of the water bath.

The semi-conductor temperature transducers were set up by being immersed in water whose temperature was accurately measured with a precision PRT (Guildline 9535). The responses of the temperature sensors were considered linear over the desired measuring range and therefore only required to be set up at two different temperatures.

The quantum sensor was compared with a recently calibrated unit at various quantum flux densities and a new calibration found. The amount of direct radiation entering through the top surface of the chamber was measured by placing a quantum sensor inside the chamber and comparing the measurement with a quantum sensor outside at various quantum flux densities. The object of the experiment was to estimate the quantum flux density that would actually reach the plant material inside the chamber at varying ambient quantum flux densities. The results revealed that the glass top of the chamber reduced the amount of direct radiation by 7% on average.

The flowmeter was calibrated using the soap bubble technique (Levy, 1964), and was corrected for dry air at 20 ^{o}C and atmospheric pressure. The flow was measured with the tubing and drying tube attached to the porometer to include any effects of their resistance. The flowmeter calibration was also frequently checked with a mass flowmeter as a quick alternative to the soap bubble technique.

3.5 Functional tests

The Binos and diffusion porometer together were first tested as a CO_2 porometer under laboratory conditions, using a small amount of soda lime inside the chamber as a sink for CO_2. It was possible to balance the CO_2 concentration inside the chamber against the ambient CO_2 concentration by introducing air from a cylinder containing 100 $\mu mol\ mol^{-1}$ higher CO_2 concentration than ambient. A steady state was obtained with the balance lasting for several minutes. The repeatability of the method was demonstrated by changing the flow and rebalancing. Several different operators rebalanced the CO_2 concentrations within $\pm$ 2 % of the original flow rate. During these experiments it was assumed that CO_2 absorption by the soda lime remained constant for the short periods of use.

The CO_2 porometer operates as a semi-closed system with CO_2-enriched air being added to the volume of air in the chamber and associated tubing, with resultant leakage of air out of the chamber at the same rate as addition. The flow rate needed to balance a particular rate of absorption should therefore be inversely proportional to the difference between the balance point CO_2 concentration and the balancing gas CO_2 concentration (equation 1.1), and the calculated rate of CO_2 flux should not be flow rate dependent. This was tested by using soda lime in the porometer chamber as a constant sink for CO_2. The CO_2 concentration of the balancing gas was kept constant but the balance point was varied above and below the ambient CO_2 concentration. Fig. 3.4, shows that the resulting flow rates when the system was balanced were inversely proportional to the difference in CO_2 concentrations between balance point and balancing

gas. Changing the balance point had the same effect as changing the balancing gas concentration, thus demonstrating that the concentration of the balancing gas is not critical as long as it is known accurately. The experiment involved a range of flow rates from 5 to 25 $cm^3\ s^{-1}$, and showed that over this range there was no significant difference in the calculated rate of CO_2 absorption at the balance points.

Experiments were also carried out on tree saplings in growth rooms and in greenhouses before testing in the field. The response of CO_2 influx to quantum flux density of a shoot of Sitka spruce is shown in Fig. 3.5. The porometer chamber enclosing the shoot was illuminated from above by a high pressure mercury vapour discharge lamp (Wotan HQI 400W), through a water bath to reduce infra-red radiation. The quantum flux density was varied by interposing layers of neutral density muslin. The shoot was equilibrated at the highest quantum flux density for two hours before the quantum flux density was reduced in steps, a measurement of CO_2 flux being made at each stage. A typical light response curve was obtained with appropiate rates of photosynthesis.

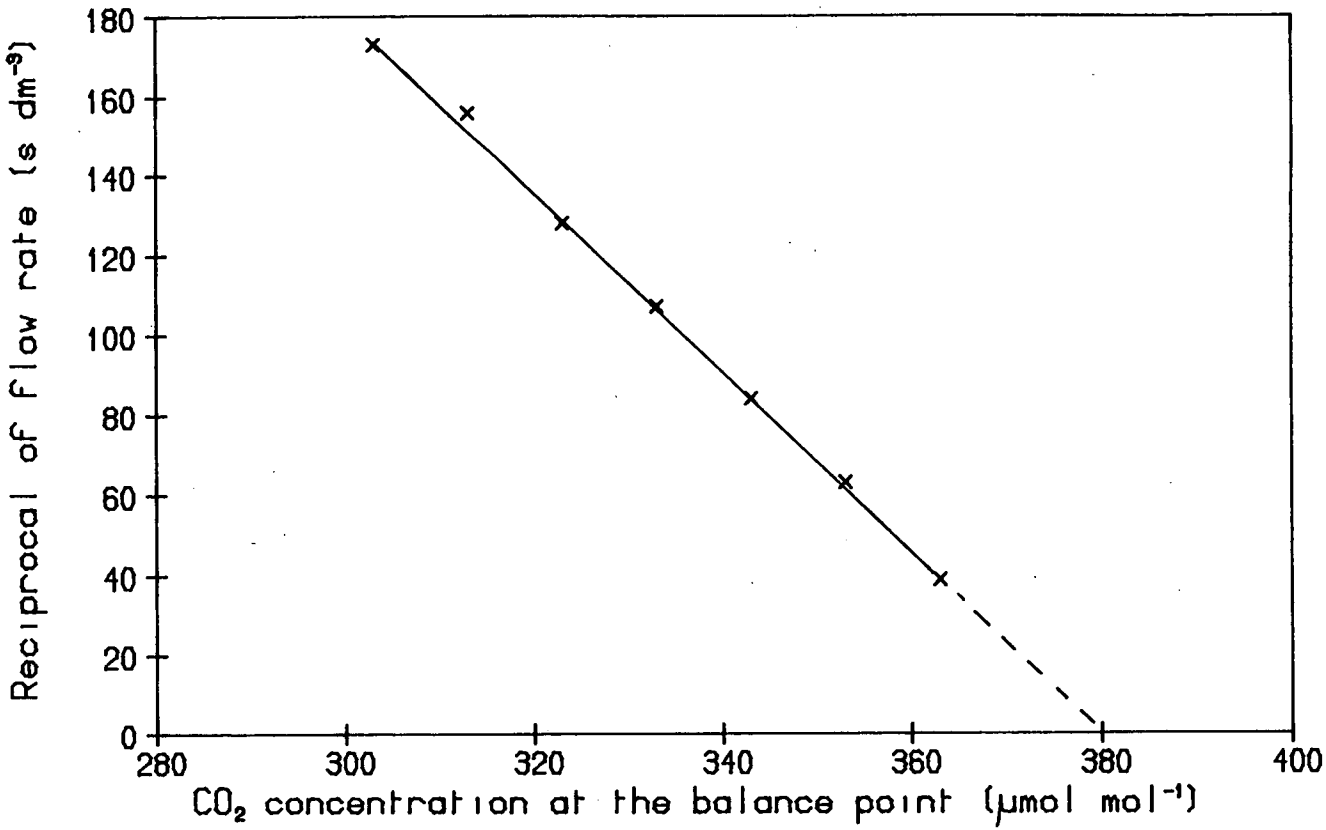

Fig. 3.4. Relationship between the reciprocal of the volume flow rate of the balancing gas into the porometer chamber and the CO_2 concentration selected as the balance point. The chamber contained soda lime to provide a constant sink for CO_2. The concentration of CO_2 in the balancing gas was 380 umol mol^{-1}.

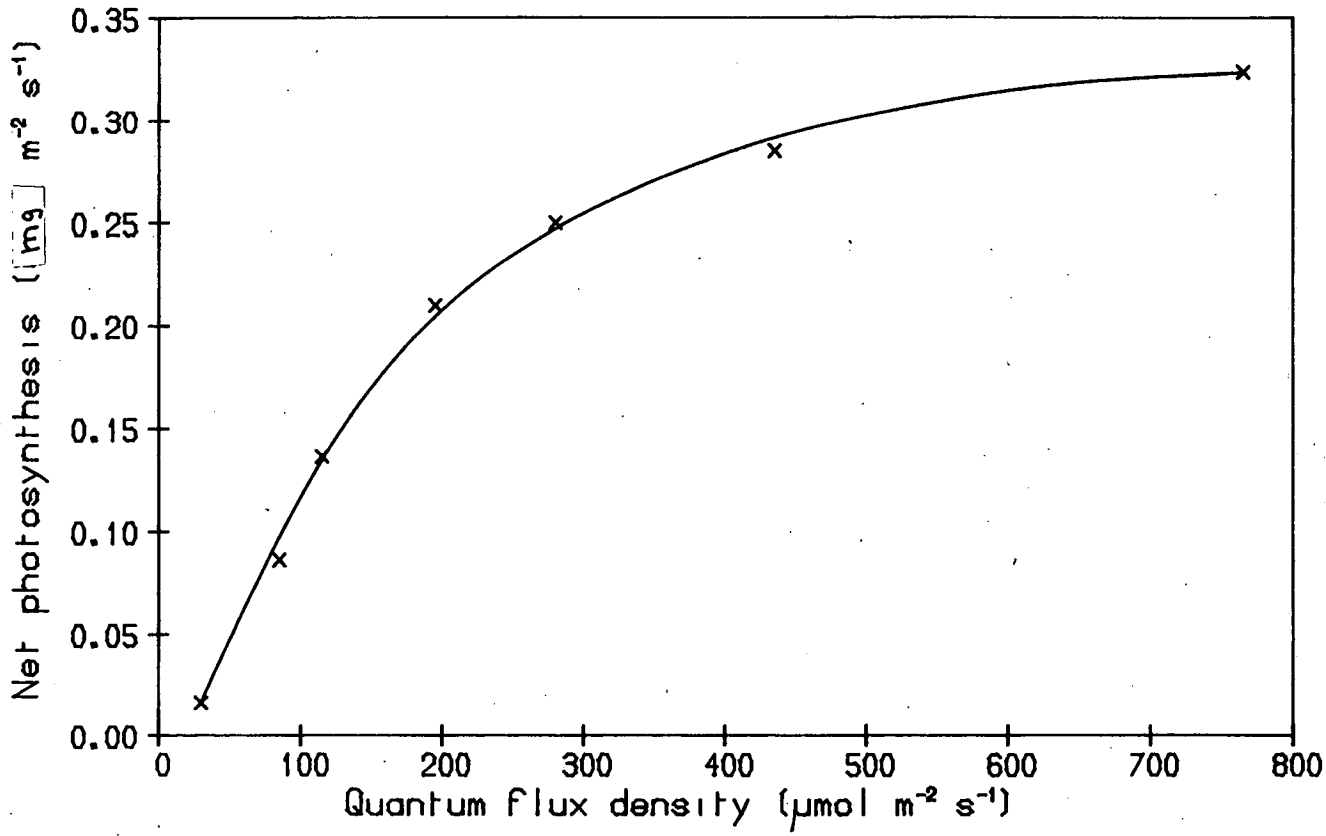

Fig. 3.5. Relationship between rate of net photosynthesis and quantum flux density for Sitka spruce measured with the null balance CO_2 porometer using the differential channel for balancing. Ambient CO_2 concentration 345 μmol mol^{-1}; temperature 21 ^{o}C; vapour pressure deficit 1.62 kPa.

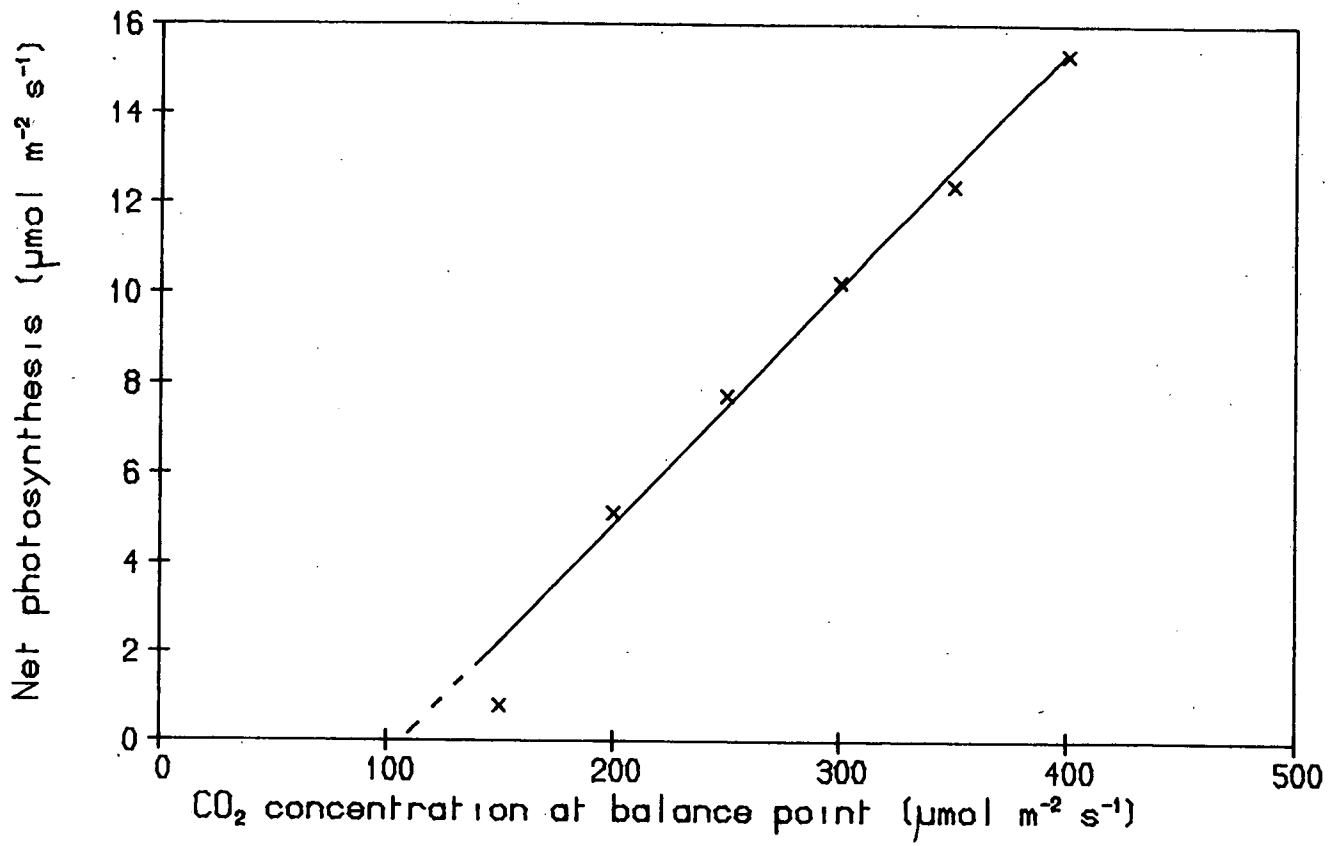

Fig. 3.6. Relationship between rate of net photosynthesis and CO_2 concentration for Scots pine measured with the null balance porometer using the absolute channel for balancing. Incident quantum flux density in the chamber 580 µmol m^{-2} s^{-1}; temperature 26.5-27.9 ^{o}C; vapour pressure deficit 1.71-1.85 kPa.

Fig. 3.6 shows the effects of balancing at different CO_2 concentrations on the CO_2 flux of a shoot of Scots pine (Pinus sylvestris L.). To reduce the CO_2 concentration in the chamber to 150 μmol mol^{-1} quickly, the system was flushed briefly with CO_2-free air. The experiment began at the lowest CO_2 concentration, the balance point being increased in steps with approximately 10 minute intervals between each measurement. The shoot and chamber were illuminated as before with a constant quantum flux density of 580 μmol m^{-2} s^{-1}. In this experiment balancing was carried out using the absolute channel since the balance point concentrations were outside the range of the differential channel. A typical CO_2 response curve was obtained, emphasising the importance of knowing the balance concentration.

3.6 Chamber design

The original chamber was constucted as described previously and ventilated by a small fan (Micronel V241L) with an air flow of 90 l min^{-1}. The air flow within the chamber was investigated with a small hot wire anemometer and was found to give an average value of 0.7 m s^{-1} throughout the chamber.

Leaf temperatures of broad-leaves may be easily measured with a small sensor in contact with the surface, but this technique is not feasible when working with conifers. Consequently, it was assumed in calculations of stomatal conductance that the leaf was at the same temperature as the chamber air that was measured. Therefore tests were carried out to investigate the distribution of temperature within the chamber.

The experiments were carried out inside a large growth cabinet with high intensity lighting, a constant cabinet air temperature of 20 °C, and horizontal air speed of 0.6 m s^{-1}. Temperature differences were

measured using fine gauge (0.3 mm) thermojunctions attached to the chamber wall, to the non-sensing surface of the vaisala humidity sensor and to a needle on a prepared Sitka spruce shoot. The thermojunctions were all referenced to the air in the duct below the main chamber, through which the air is drawn by the mixing fan. This position is normally the site of the porometer temperature sensor, and is well ventilated and shielded from direct radiation. An absolute measure of chamber air temperature was provided by another similarly placed thermojunction that was referenced to a shielded and ventilated precision PRT measuring cabinet air temperature. The thermocouples were connected to microvoltmeters and chart recorders that had previously been zeroed and calibrated.

Measurements were first taken with the chamber open and fan on and with all the lights in the growth cabinet on. After a steady state had been reached, the chamber was closed around the shoot and changes in temperature recorded with respect to time. When a steady state had again been reached, the irradiance was reduced by switching off certain lamps, and the effects recorded. Measurements were taken at six different irradiances and also in darkness.

Fig. 3.7 shows that the growth cabinet air temperature remained constant at 19 $\pm$ 0.5^{o}C, irrespective of irradiance, but that the air temperature inside the chamber was almost a linear function of irradiance reaching 28 ^{o}C at the highest irradiance. Fig. 3.7 also shows there was little difference in temperature between chamber wall and chamber air and that this remained constant, except in darkness where there was no difference. Fig. 3.8 shows that at the highest irradiance, the needle temperature was 0.9 ^{o}C warmer than chamber air, whilst the Vaisala sensor was 0.6 ^{o}C cooler. Thus there was a needle-Vaisala sensor temperature difference of 1.5 ^{o}C. This

difference was approximately a linear function of irradiance, and was apparent soon after chamber closure within one minute. Fig. 3.9 shows the error in stomatal conductance, with respect to relative humidity and various leaf-Vaisala temperature differences. The error in conductance becomes larger at higher relative humidities and at lower Vaisala sensor temperatures. If the needle temperature were assumed to be the same as that of the Vaisala sensor, a 1.5 ^{o}C difference would lead to an overestimation of stomatal conductance by 24.2 % (Fig. 3.9) at a Vaisala sensor temperature of 20 ^{o}C and relative humidity of 60 %.

An attempt was therefore made to reduce this error by redesigning the chamber to minimise these internal temperature differences. A new chamber was constructed of 3.3 mm thick polymethylpentene (PMP,TPX; Mitsui plastics). This material has very low water vapour absorption and excellent light transmission properties and is more readily available than cross-linked polystyrene. However, there are no suitable bonding agents for this plastic so the chamber was screwed together with 1.5 mm nickel plated screws, the joints being sealed with a gasket of RTV silicon rubber adhesive. The new chamber was larger with internal dimensions of 85 mm x 70 mm x 100 mm. It was constructed in two halves with a closed cell polyethylene foam seal (Kwikstik Inseal) on the abutting surfaces (Fig. 3.10). A larger and more powerful fan (Micronel V466M) was supported in the centre of the chamber and had a capability for moving 220 l min^{-1} and gave an average air velocity of 1.5 m s^{-1}. The Vaisala sensor was positioned well into the air flow path just above the fan blades. The fan drew air from the top of the chamber through the shoot and past the Vaisala sensor to the bottom of the chamber before recirculating it up the sides of the chamber.

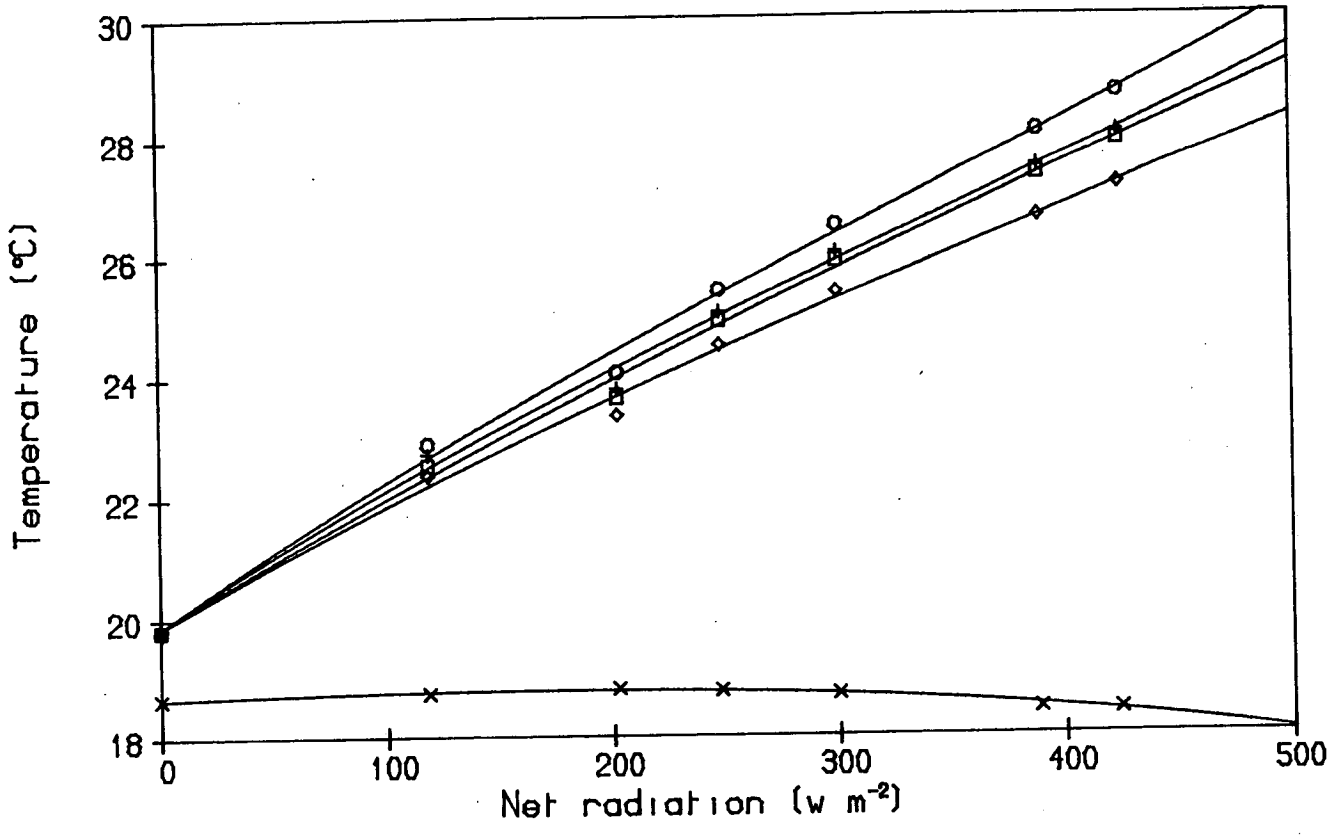

Fig. 3.7. Investigation of temperature within the original chamber carried out in a growth cabinet at various irradiances and darkness; (—×—) growth cabinet air temperature; (—◇—) vaisala sensor temperature; (—□—) chamber wall temperature; (—+—) chamber air temperature; (—○—) Sitka spruce needle temperature. Growth cabinet horizontal air speed 0.6 m s^{-1}.

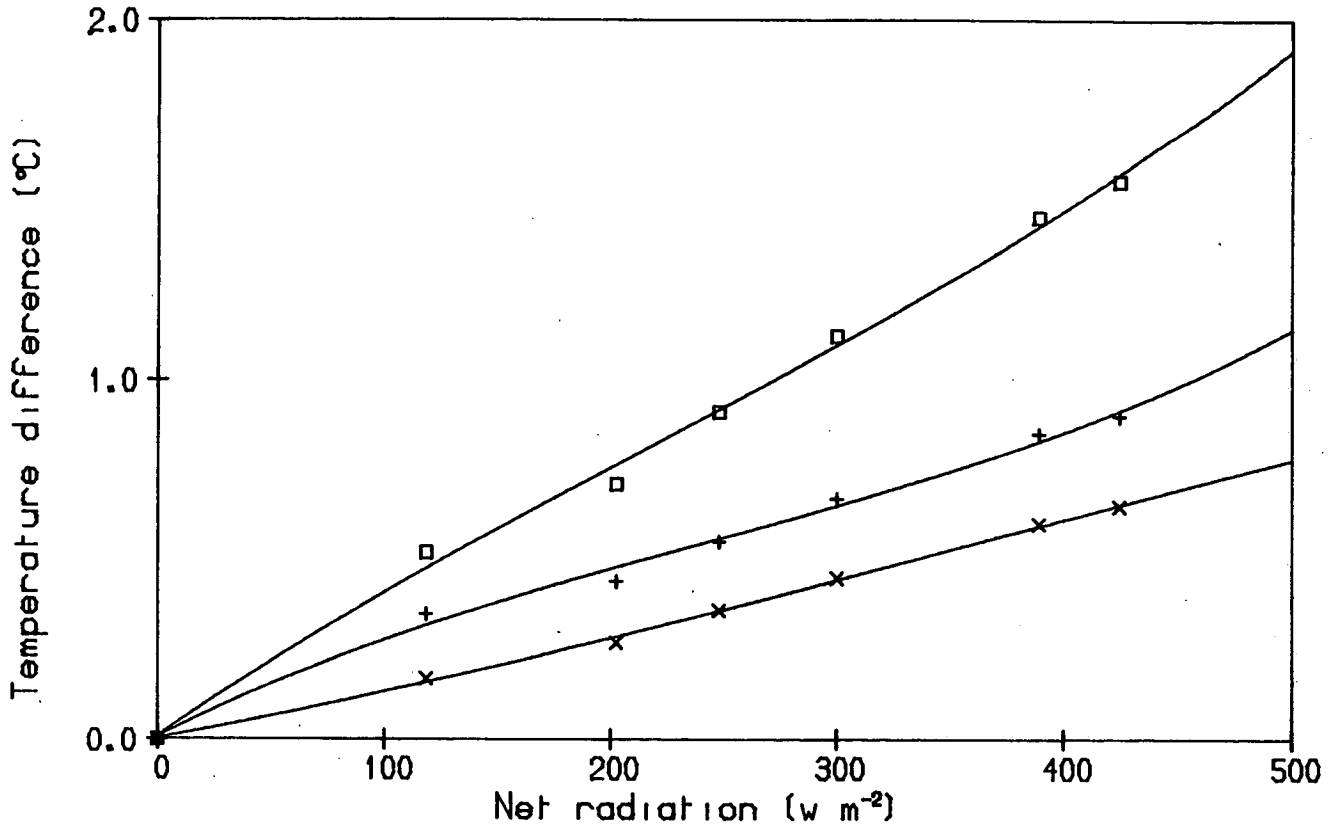

Fig. 3.8. Temperature differences within the original chamber at various irradiances and darkness, measured in a growth cabinet with a horizontal air speed of 0.6 m s^{-1}; (—×—) needle-chamber air temperature difference; (—+—) chamber air-vaisala sensor temperature difference; (—⊟—) needle-vaisala sensor temperature difference.

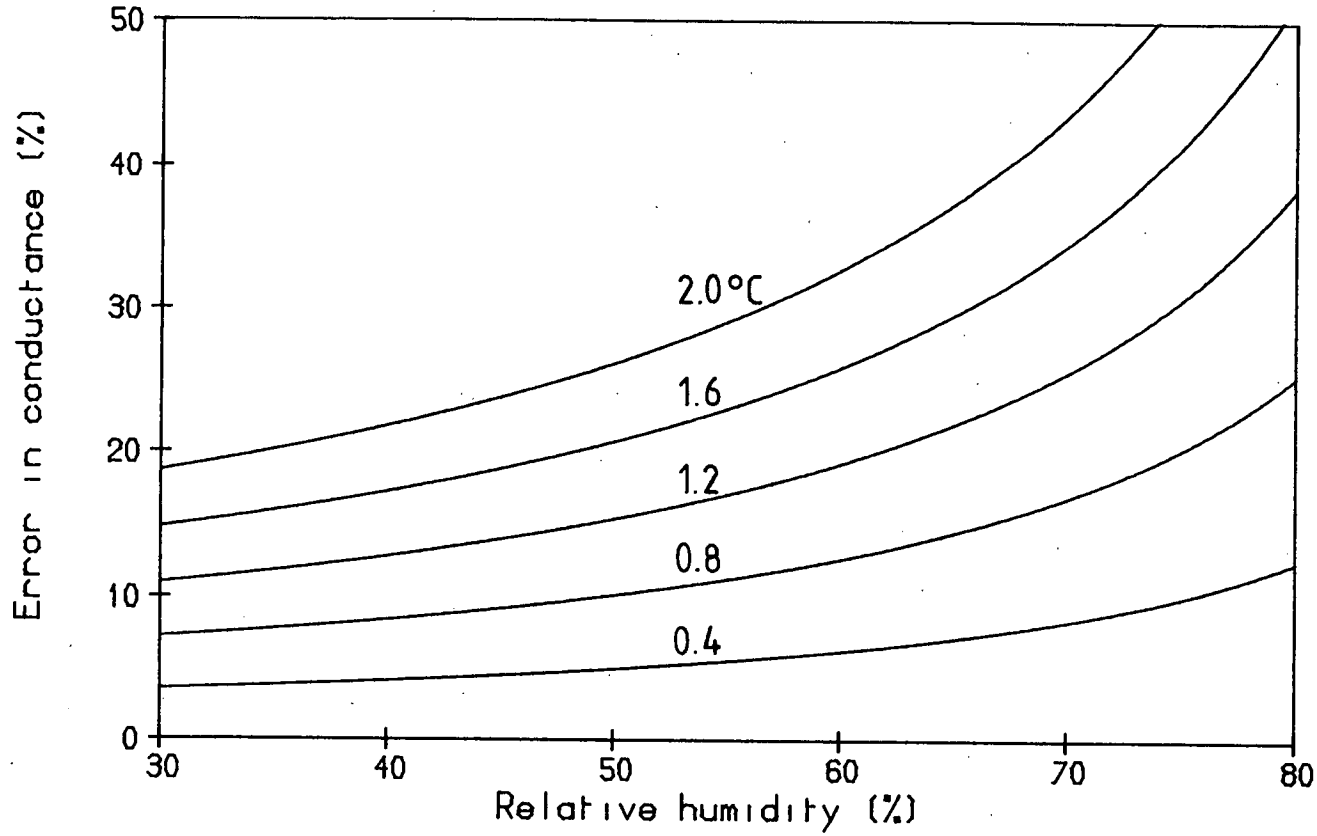

Fig. 3.9. Calculated % errors in estimation of stomatal conductance at an chamber air temperature of 20 °C over a range of relative humidities normally experienced in the field; for various needle-vaisala sensor temperature differences.

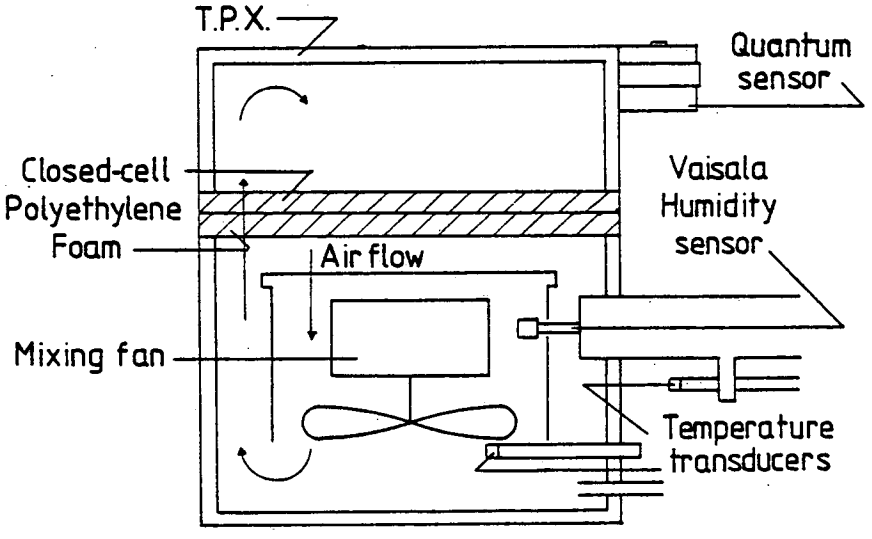

Fig. 3.10. A diagram of the modified porometer chamber in cross-section.

The new chamber was tested in a similar way as the old chamber, but only at the highest irradiance since the temperature differences were linearly related to irradiance. The improved air circulation inside the chamber resulted in more uniform conditions with smaller temperature differences. The Vaisala sensor was 0.09 ^{o}C cooler than the circulating air and the needle was 0.8 ^{o}C warmer than the Vaisala sensor. At a Vaisala sensor temperature of 20 ^{o}C and relative humidity of 60 %, a temperature difference of 0.8 ^{o}C would lead to an overestimation of stomatal conductance by 12.7 %, if the needle temperature were assumed to be the same as that of the Vaisala sensor.

At the highest radiation load the air inside both cuvettes was approximately 9 ^{o}C warmer than the ambient cabinet air, after a period of 20 minutes. When used in the field the chamber is rarely kept on the same shoot for more than 5 minutes. However the leaf-Vaisala sensor difference is the important factor and this is attained shortly after chamber closure. This difference was reduced by half by greatly increasing the air circulation in the chamber at the sacrifice of increasing the chamber volume slightly and hence reducing the sensitivity of the system. Any further increase in air movement may detrimentally affect the leaves with little gain in temperature uniformity.

The error can, however, be further reduced to insignificance by keeping the chamber out of direct sunlight during measurements of stomatal conductance in the field. It is also desirable to leave the chamber open and in the shade inbetween measurements.

CHAPTER 4

FIELDWORK

4.1 Introduction to fieldwork

Sitka spruce has been widely planted as an exotic in western Europe for 150 years since its introduction into the U.K. It is the most important species planted in the U.K. and is now considered a crop of major economic importance (Jarvis, 1981). This has led to increasing research interest into the growth response of Sitka spruce to the environment. In particular, physiological processes such as photosynthesis, respiration and stomatal action, have been studied in response to environmental factors like quantum flux density, temperature and vapour pressure deficit (Ludlow and Jarvis, 1971; Neilson et al, 1972; Turner and Jarvis, 1975; Neilson and Jarvis, 1975; Watts et al, 1976; Watts and Neilson, 1978; Beadle et al, 1978, 1979; Leverenz and Jarvis, 1979, 1980; Leverenz et al, 1982).

In a review of published papers concerned with photosynthesis and respiration of conifers (Linder, 1979) only 20 out of 410 papers involved Sitka spruce, and of these, only 7 were concerned with trees rather than saplings and only 1 was concerned with the stand. To be able to calculate the carbon balance of a tree or a forest stand it is necessary to know the variation in rate of photosynthesis in different parts of the tree crown (cf. Linder and Lohammar, 1981). The majority of photosynthetic studies have been carried out in laboratories on individual needles or shoots, where environmental conditions may be controlled with ease. The information from field measurements of gas exchange within different parts of the crown of coniferous trees is

rather limited (cf. Linder, 1979).

$^{14}CO_2$ techniques have been used in the past to measure photosynthesis of conifers in the field (e.g. Watts et al, 1976), but such methods are destructive and only allow one measurement to be made on a shoot. Infra-red gas analysis techniques are more suitable since measurements may be repeated allowing diurnal, or even seasonal changes in photosynthesis to be monitored on the same shoots. This method has been used to study canopy photosynthesis of conifers, but has required mobile laboratories (Woodman, 1971; Schulze et al, 1977; Leverenz, 1981), or permanent installations (Linder and Troeng, 1980). These techniques involve using a number of climatised assimilation chambers that may be sequentially monitored. This usually restricts the study to an intensive investigation of a few shoots because of the high costs of equipment and manpower. When studying a diverse structure such as a conifer forest canopy, it is essential to sample the main source of variation within the canopy during the same time period. The diffusion porometer has successfully been used to investigate extensively the variation in stomatal conductance throughout a canopy (Leverenz et al, 1982). This study compares an investigation of the variation in photosynthesis throughout the same forest canopy.

4.2 Site and methods

The fieldwork was carried out at the Institute of Terrestrial Ecology experimental site at Rivox, Southwest Scotland, part of the Forestry Commission Greskine forest (Nat.Grid.Ref. NT016045). The experimental area consisted of a 21 year old plantation of Sitka spruce planted in blocks of 350-400 stems at a spacing of 1 x 1.5 m, on a uniform South facing slope of 6° and at 355 m above sea level.

The site has been under investigation for a number of years so that the growth and structure of the plantation is well documented (Ford, 1976; Ford and Deans, 1977; Cochrane and Ford, 1978; Ford and Deans, 1978; Ford, 1982).

In the centre of one 20 hectare compartment, a permanent scaffolding structure has been erected to give access to the canopies of about 40 trees within a 9 m x 9 m area. The scaffolding was constructed of welded 0.05 m box section steel, to a height of 8 m, with movable platforms throughout. However the scaffolding was constructed some 10 years ago and despite an extension up to 8 m, the upper whorls of some trees could not be reached. To give free access to all parts of the canopy, up to 2 m of portable aluminium tower scaffolding could be secured anywhere on top of the existing structure.

Other facilities at the site included a prefabricated hut containing living accommodation, laboratory and workshop, a meterological station above the canopy and computer facilities for recording the meterological data. Electricity for the hut and computer was provided by generators, heating and cooking facilities were supplied with bottled gas, water was pumped from a local burn and the hut was connected to the telephone system.

The site is easily reached by Forestry Commission roads and was about 3 miles from the main road and some 60 miles from Edinburgh. To enable early morning and late evening measurements to be taken, it was necessary to live in the hut for a few days at a time.

Four sets of data were obtained relating to different shoot ages and canopy position. After initial trials at the site, measurements began at the beginning of August 1981 and work continued periodically until the middle of October, when the short days and inclement weather

made further study unprofitable. During this period, current year terminal shoots were investigated at three different whorl levels. Measurements were made on three shoots on separate branches of two similar trees at whorl levels 3, 6 and 9. The two trees investigated were intermediate in social status (Leverenz et al, 1982) with ten live whorls. Whorl 3 foliage was free from interference from neighbouring trees, whorl 6 foliage marked the position of canopy closure and whorl 9 foliage was well shaded within the canopy. The object of the investigation was to compare the rates of photosynthesis of the different whorls and eventually different needle ages.

The second set of data was obtained in 1982 over a short period of three weeks during which time the 1982 foliage developed rapidly. Eight terminal shoots were selected on whorl 4 of a tree of intermediate social status. Four of the eight shoots had the developing current year foliage removed. The effect of the developing shoots on the previous years foliage was investigated.

The third set of data was obtained from terminal current year shoots during 1982 in a similar way as in 1981 but from different trees and whorl levels. Measurements were made on two shoots on separate branches of two similar intermediate trees at whorl levels 3, 4 and 5. Whorl 3 shoots were above the point of canopy closure, whorl 4 shoots were at the transition stage and whorl 5 shoots were just below the point of canopy closure.

The fourth set of data was obtained from the same intermediate trees as used to obtain the third data set. One year old lateral shoots were measured on the same branches and whorls as the terminal shoots measured previously. The object of the investigation was to compare the rates of photosynthesis of different aged foliage at three positions within the canopy.

Before each measuring period shoots were selected to be measured and prepared by removing some needles from the branch so that the chamber would seal around the selected portion of shoot material. The shoots were prepared and labelled at least three days before measuring, to allow time to recover from any mechanical damage that may have been caused.

To make the photosynthesis measurements one person moved the chamber from shoot to shoot within the canopy while measurements were taken and recorded at ground level by another. The equipment needed in the field consisted of: the null-balance diffusion porometer control unit with 10 m of cable and tubing to connect it to the chamber, the Binos infra-red gas analyser and 3 m of tubing to and from the chamber, a large plastic dustbin that acted as an air resevoir to dampen out any fluctuations in ambient CO_2 concentration, small aluminium cylinders containing a range of dry CO_2 enriched air, two 26 ampere-hour batteries (Varley 12.15/30), a solarimeter (Kipp and Zonen CM3) and integrating unit (Delta-T Devices MV1), and an Assmann ventilated pyschrometer (Casella). With the exception of the dustbin, cylinders and batteries, the rest of the equipment fitted into an environmentally protected aluminium case measuring 0.87 x 0.47 x 0.37 m. The equipment could be transported from a vehicle to the experimental site in two trips by two people. Once at the site, the equipment could be set up and be operational in under 15 minutes if the Binos gas analyser was at its operating temperature.

When travelling to the forest, power was supplied to the Binos so that it had warmed up on reaching the site. When staying in the forest overnight, the Binos was connected to the generator power supply and switched on, by means of a time clock, two hours before measurements were to begin in the morning. The CO_2 porometer was operated as

described previously with periodic checks on the zero points of both flowmeter and quantum sensor since they were slightly sensitive to ambient temperature. Measurements usually began in the early morning if the shoots were dry, and continued throughout the day until light levels made further investigation unprofitable. Up to 18 shoots were measured in any one period, usually with a break in between each set.

Irradiance was recorded periodicaly throughout the day and the relative humidity of the ambient air was measured with a ventilated Assmann physchrometer at a point within the canopy at the beginning and end of each set of measurements. These independent measurements provided a check on the calibration of the Vaisala sensor and also provided basic meterological data when the automatic weather station was not operating.

CHAPTER 5

DATA ANALYSIS

5.1 Objectives

The objective of the fieldwork was to investigate the spatial distribution of photosynthesis within the canopy. The rate of photosynthesis of a shoot within a forest canopy is dependent on environmental variables such as light, temperature, ambient CO_2 concentration and vapour pressure deficit as well as on physiological properties of the shoots. Thus to compare data obtained from different populations of shoots, account must be taken of the environmental conditions at the time of measurement, in order to distinguish differences attributable to physiological properties of the shoots.

The photosynthetic response of Sitka spruce to environmental variables has been investigated in the laboratory where one variable may be changed while other important variables are kept constant or non-limiting (Ludlow and Jarvis, 1971). Under field conditions many environmental variables tend to fluctuate together and are strongly correlated resulting in compound effects. Fig. 5.1 shows rate of net photosynthesis plotted against quantum flux density for current year shoots on whorl 4 of two trees. There was an obvious relation between net photosynthesis and quantum flux density but the apparent variation was such that this could not be compared quantitatively with data from a different population. Therefore there was a need to describe the data with some form of mathematical function that would take account of more than one variable acting at a time.

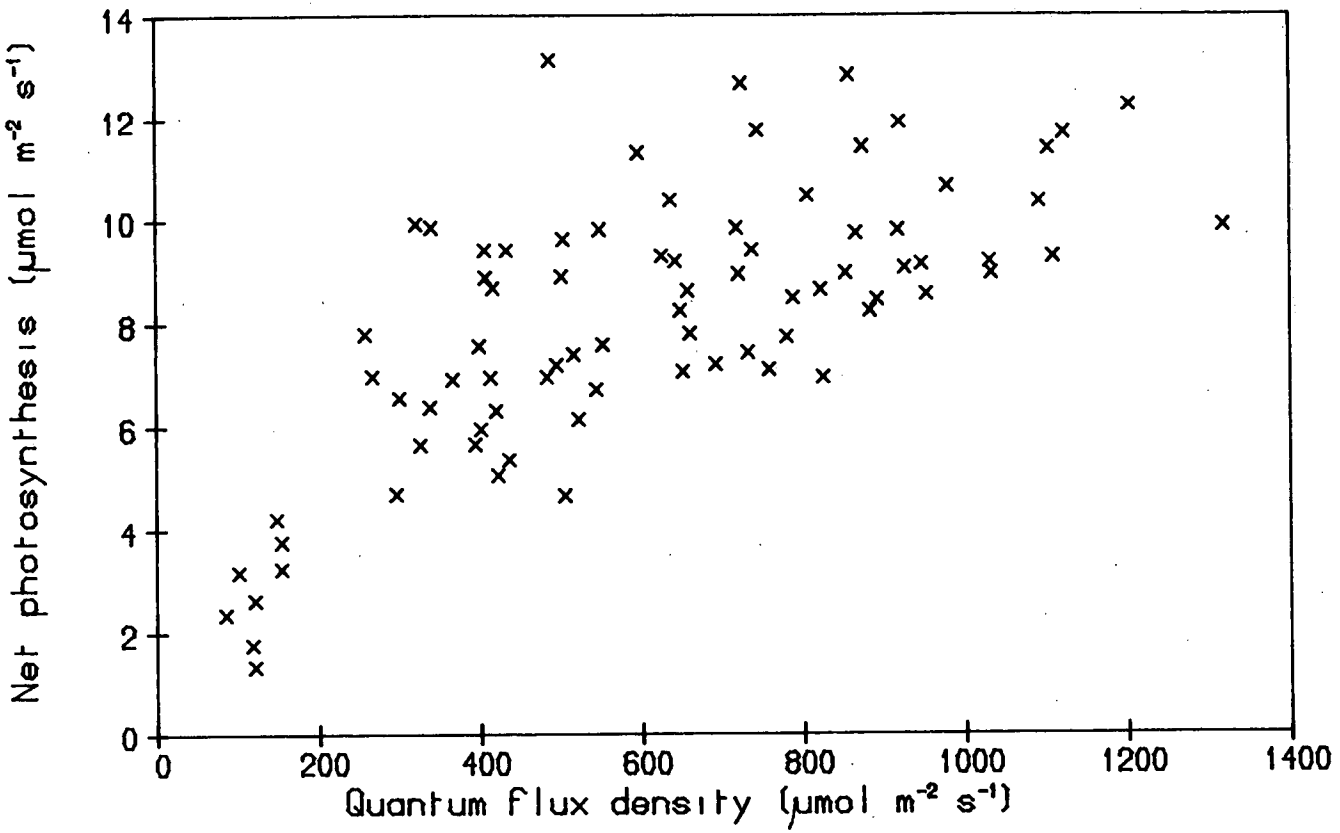

Fig. 5.1. Relationship between net photostnthesis and quantum flux density for eight current year shoots on whorl 4 of two trees.

5.2 Rectangular hyperbola

The response of phototsynthesis to quantum flux density is commonly described as a rectangular hyperbola (de Wit, 1965; Procter et al, 1976; Thorpe et al, 1978). A rectangular hyperbola was fitted to the data by means of an iterative, non-linear least squares regression package that estimated parameter values by systematically changing the initial values until there was no further reduction in the residual sum of squares (BMDP PAR). The parameter estimates were assumed to have converged on the true parameter values. The function had the form:

$$F_n = a*Q*Fm/(a*Q + Fm) \qquad (5.1)$$

where:

F_n is the rate of net photosynthesis (μmol m^{-2} s^{-1}),

a is the initial slope of the light response curve,

Q is the quantum flux density (μmol m^{-2} s^{-1}),

Fm is the asymptotic rate of photosynthesis at saturating quantum flux density (μmol m^{-2} s^{-1}).

Fig. 5.2 shows the rectangular hyperbola function fitted to the data of Fig. 5.1. The fitted curve has an initial slope of 0.046, and an asymptote of 13.1 μmol m^{-2} s^{-1}. By comparing the predicted rates of net photosynthesis with observed values, it is possible to get a value of the mean square error (mse) and an estimate of the amount of variability accounted for. In this case these were 2.27 and 66% respectively. Some of the variability not accounted for in the function may be a result of the influences of variables such as stomatal conductance and temperature. Alternatively the function may not be completely appropriate since it predicts responses that pass

through the origin. The estimates of stomatal conductance for this set of data varied between 0.054 and 0.285 mol m^{-2} s^{-1}, with an average value of 0.120 mol m^{-2} s^{-1}, and the temperature inside the chamber varied between 17.7 and 31.9 ^{o}C, with an average value of 26 ^{o}C. By either selecting data with stomatal conductances between 0.09 and 0.15 mol m^{-2} s^{-1}, or by selecting data with chamber temperatures between 24 and 28 ^{o}C, the mean square error was reduced to 1.61 and 76% of variation could be accounted for by fitting a rectangular hyperbola. However this approach reduced the number of data points available for analysis and this may have influenced the fit of the function.

The technique of fitting a mathematical function to data in an attempt to describe the distribution, has been referred to as modelling, with the function called the model. Various types of model have been used to describe photosynthesis ranging from simple models, such as the rectangular hyperbola, to complex multi-parameter functions that take into account many variables (Thornley, 1976).

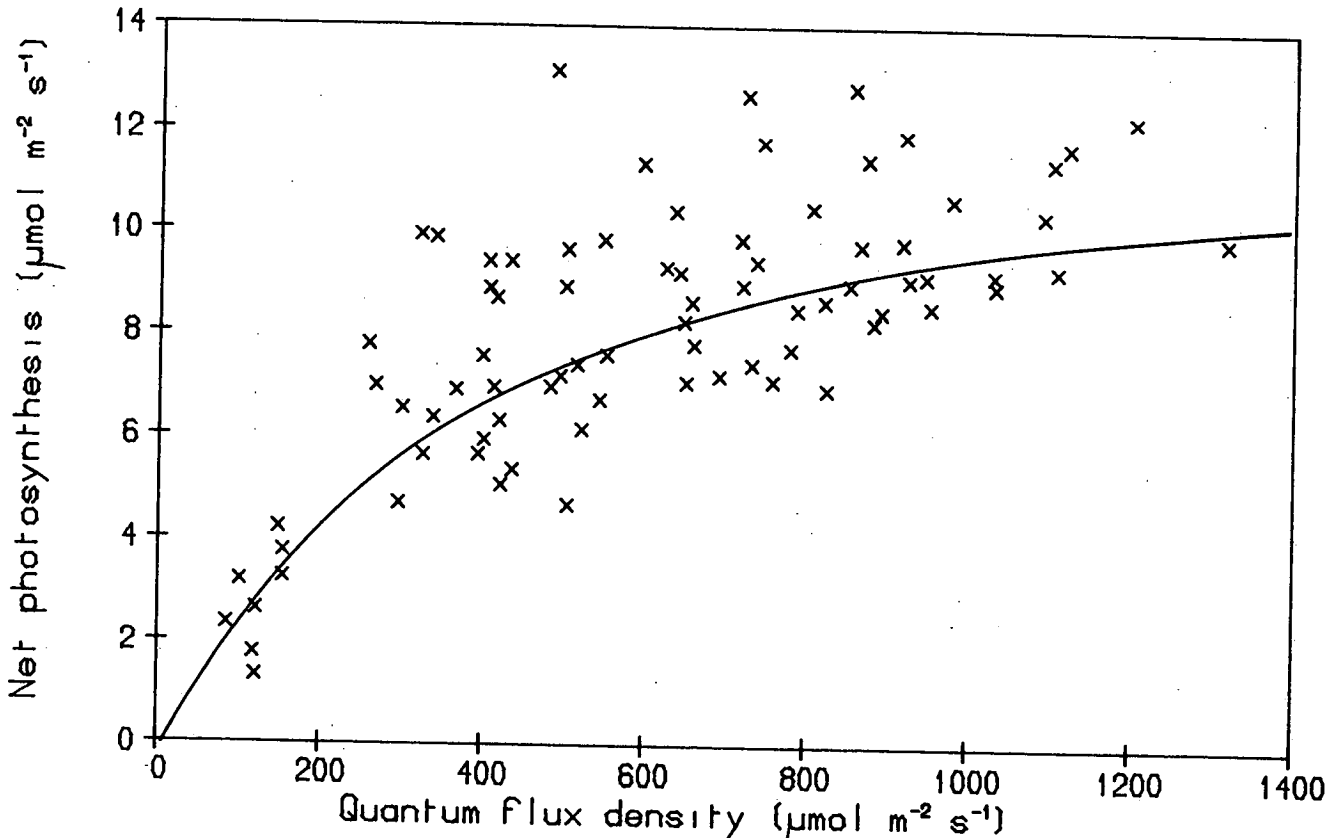

Fig. 5.2. A rectangular hyperbola function fitted to the data of fig. 5.1.

5.3 Non-rectangular hyperbola

In an attempt to improve the description of the data, a more complex model that took into account the influence of stomatal conductance was used (Miranda, 1982). Although a rectangular hyperbola is commonly used to describe the response of photosynthesis to quantum flux density, a non-rectangular hyperbola has been shown to represent the relationship better at low levels of quantum flux density (Prioul and Chartier, 1977; Goudriaan, 1978), especially in conifers (Leverenz, 1979). A non-rectangular hyperbola representing the relationship of photosynthesis to quantum flux density is:

$$M*F^2 - (a*Q + Fm)F + a*Q*Fm = 0 \qquad (5.2)$$

where:

F is the CO_2 flux (μmol m^{-2} s^{-1}),

Q is quantum flux density (μmol m^{-2} s^{-1}),

Fm is the asymptotic rate of photosynthesis at saturating quantum flux density (μmol m^{-2} s^{-1}),

M is the convexity parameter,

a is the initial slope of the light response curve.

The parameter M, is the convexity parameter or coefficient which determines the non-rectangularity of the function. It may have values ranging from 0 to 1, where 0 results in a rectangular hyperbola and 1 results in an extreme non-rectangular hyperbola of two straight lines (the Blackman response function).

In terms of the flux of CO_2 through the stomata:

$$F = F_n + R_d \qquad (5.3)$$

and $F_m = F_{nm} + R_d$

where:

R_d is the rate of dark respiration ($\mu mol\ m^{-2}\ s^{-1}$).

For field data, it is adequate to assume a linear relationship between F_{nm} and C_i with a slope of g_m:

$$F_{nm} = g_m(C_i - G) \qquad (5.4)$$

where:

g_m is the mesophyll conductance ($mol\ m^{-2}\ s^{-1}$),

C_i is the intercellular space CO_2 concentration ($\mu mol\ mol^{-1}$),

G is the CO_2 compensation point ($\mu mol\ mol^{-1}$).

The intercellular space CO_2 concentration (C_i) may be described as:

$$C_i = Ca - (F_n/g_s) \qquad (5.5)$$

where:

C_a is the ambient CO_2 concentration ($\mu mol\ mol^{-1}$),

g_s is the vapour phase conductance for CO_2 ($mol\ m^{-2}\ s^{-1}$). In the stirred porometer chamber, the boundary layer resistance can be regarded as negligible so that g_s can be equated with the stomatal conductance and is obtained by dividing the stomatal conductance for water vapour by 1.606.

Combining equations, 5.4 and 5.5 gives:

$$F_{nm} = [C_a - (F_n/g_s) - G]g_m \qquad (5.6)$$

Combining equations 5.2, 5.3 and 5.6 gives:

$$[M + (g_m/g_s)]F_n^2 + ([2M + (g_m/g_s)]R_d - [1 - (g_m/g_s)]a*Q - (C_a - G)g_m)F_n + a*Q[(C_a - G)g_m] + [R_d*M - a*Q - ((C_a - G)g_m)]R_d = 0 \qquad (5.7)$$

Equation 5.7 has a quadratic form $\alpha X^2 + \beta X + \gamma = 0$ and can therefore

be solved for F_n using the equation:

$$F_n = [-\beta - (\beta^2 - 4\alpha\gamma)^{0.5}]/2\alpha \quad (5.8)$$

where:

$$\alpha = M + (g_m/g_s) \quad (5.9)$$

$$\beta = [2M + (g_m/g_s)]R_d - [1 + (g_m/g_s)]a^*Q - (C_a - G)g_m \quad (5.10)$$

$$\gamma = a^*Q^*g_m(C_a - G) + [R_d^*M - a^*Q - (g_m(C_a - G))]R_d \quad (5.11)$$

Equation 5.7 expresses net photosynthesis (F_n), in terms of quantum flux density (Q), ambient CO_2 concentration (C_a), stomatal conductance for CO_2 (g_s), mesophyll conductance for CO_2 (g_m), dark respiration (R_d), CO_2 compensation point (G), convexity coefficient (M), and initial slope of the light response curve (a). Of these variables, Q, C_a and g_s can be derived from the field data, the other variables may be estimated as parameters by solving the equation with observed values of F_n and g_s, or be assigned values derived from laboratory experiments. Function 5.7 was fitted to the whorl 4 data used before to estimate values for the parameters, and gave a mean square error of 1.26 which accounted for 82% of the variation.

Although the function appeared to be a better description of the data, some of the parameter estimates were unrealistic when compared to laboratory derived estimates. In particular the convexity parameter was estimated as 0, and the mesophyll conductance was estimated as 0.1 mol m^{-2} s^{-1}. To obtain unbiased estimates of the parameters it is necessary to have data that are evenly distributed with respect to the input variables. In the case of the response of photosynthesis to quantum flux density, there should be an equal amount of data for photosynthesis at high quantum flux and high stomatal conductance as for photosynthesis at high quantum flux and low stomatal conductance.

The same applies to the response of photosynthesis to other variables such as ambient CO_2 and temperature. However, it is very unlikely that an even distribution of data will be obtained when input variables are highly correlated such as in the case of quantum flux density and temperature. Fig. 5.3 shows temperature as a function of quantum flux density and demonstates the high degree of correlation. Parameters such as a, G and R_d are directly influenced by the proportion of measurements made at low quantum flux densities between 0 and 200 $\mu mol\ m^{-2}\ s^{-1}$.

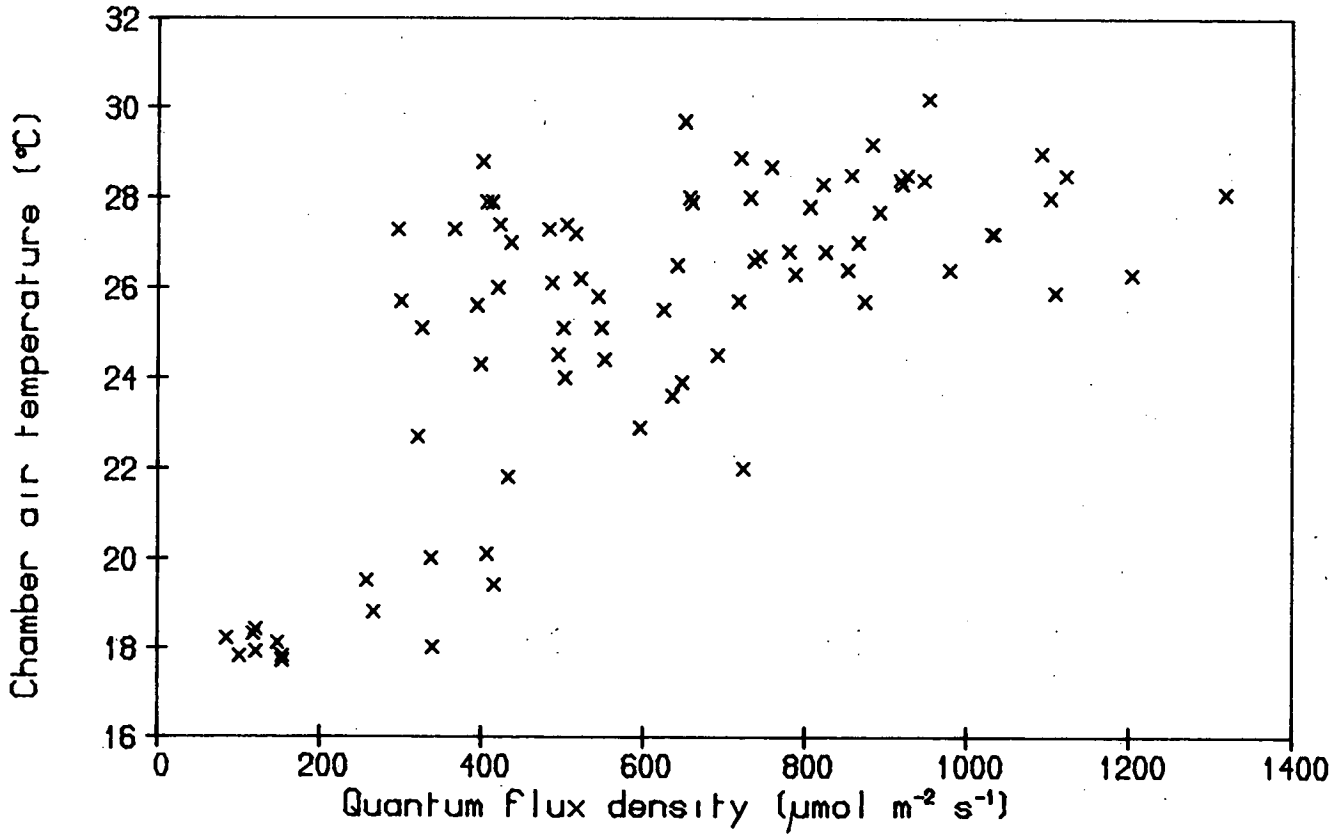

Fig. 5.3. Relationship between porometer chamber air temperature and quantum flux density for measurements made on current year shoots on whorl 4 of two trees.

The non-linear regression package used required initial estimates, as well as maximum and minimum values, for each of the parameters. The mean square error could be reduced by removing the constaints on the parameters but biologically significant parameters such as R_d and g_m could lose their relevance. In an attempt to improve the parameter estimations, function 5.7 was fitted to the whorl 4 data with R_d fixed at a value of 1.0 μmol m^{-2} s^{-1} and G fixed at 50 μmol mol^{-1}. The resulting mean square error was 1.25 and the fitted curve accounted for 82% of the variability. The fit was slightly better than before and the estimated value for g_m was within the range observed for similar shoots under laboratory conditions. By fixing other parameters the fit of the function was not improved.

Some of the parameters may not be predicted as accurately as others because of the spread of data, consequently it is useful to know the relative sensitivity of the function to each of its parameters. This was tested by predicting photosynthesis from typical values for Q, C_a and g_s, along with values for each parameter that were systematically changed from -50% to +50%. Each predicted photosynthesis rate was expressed as a percentage of the value when all the parameters were unchanged. Fig. 5.4 shows the sensitivity of function 5.7 to each of the parameters. It can be seen that the function is most sensitive to g_m. Changing g_m by +10% results in a change in predicted photosynthesis by +8%. The other parameters were less important causing less than 10% change in predicted photosynthesis for a 50% change in the parameter. With the exception of G and R_d, a positive increase in parameter value resulted in an overestimation of photosynthesis. It is also useful to plot the residuals of observed and predicted values of photosynthesis against the observed values. In

a good fit of the model to the data there should be an even spread of data points about the residual zero, throughout the range of photosynthesis measured. If a function is not appropriate to a particular data set, the residual analysis may demonstrate this as systematic clumping of the residuals. Fig. 5.5 shows a residual analysis of whorl 4 data fitted to function 5.7 with G and R_d fixed. The residuals are fairly evenly distributed with a slight tailing of residuals at the upper values of observed photosynthesis. This may have been due in part to the scarcity of data at high rates of photosynthesis.

However, the usefulness of a function often lies in its ability to predict as well as describe a particular data set. The validity and usefulness of a function may be tested with two similar data sets. The function is fitted to one data set to obtain the parameter estimates which in turn are used with the function and a second data set, to predict rates of photosynthesis. The predicted values may then be compared statistically with the observed values of the second data set to test the validity of the function. Validation as described was carried out on a data set consisting of eighty separate measurements which were divided into two sets by taking alternate observations. The function accounted for 80% of the variation when fitted to the second data set using parameter estimates derived from the first data set. The fit was not improved when parameters estimated from the second data set were used. This demonstrated that the function was a reasonable description of the data and indicated that it would be useful in predicting photosynthesis.

The function and its derived parameter estimates were considered as a satisfactory description of the response of photosynthesis to quantum flux density for a population of shoots. Using the function

and estimated parameter values, the response of photosynthesis may be predicted over a range of quantum flux densities. Fig. 5.6 shows the predicted curve for the whorl 4 data used previously. The responses of different populations could be assessed by either comparing biologically meaningful parameters such as a and g_m, or by comparing light response curves directly. However, direct comparison of parameters or light response curves, may not be adequate to distinguish subtle differences. Therefore statistical analyses were carried out on the parameter estimates of populations to test for significant differences. To compare two populations the function was fitted to the pooled data from both sets and to each set individually. If the mean square error was not reduced by pooling the data, the populations were considered different. This was tested statistically by carrying out an analysis of variance. The resulting variance ratio could be used to determine the probability of the populations being different (Ross, 1981).

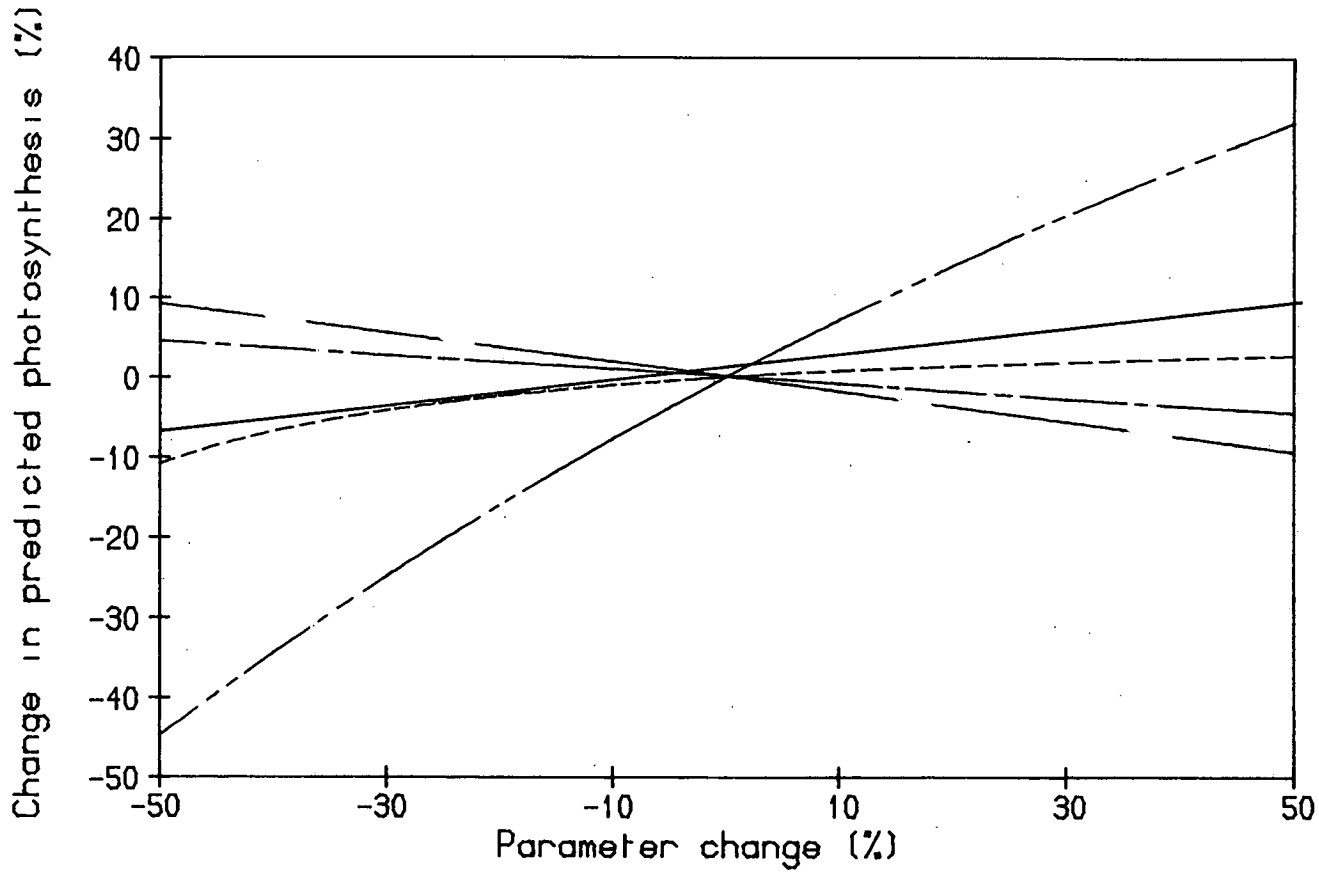

Fig. 5.4. Calculated % change in estimated net photosynthesis as individual parameters vary from minus to plus 50% their initial values; (———) M initial value = 0.8; (– – –) a initial value = 0.06; (- - - - -) gm initial value = 0.05 mol m^{-2} s^{-1}; (— - —) Rd initial value = 1.0 µmol m^{-2} s^{-1}; (— — —) G initial value = 50 umol mol^{-1}. Net photosynthesis = 8 8.24 µmol m^{-2} s^{-1}, with parameters at their initial values and gs = 0.12 mol m^{-2} s^{-1}, Q = 500 µmol m^{-2} s^{-1} and Ca = 320 µmol mol^{-1}.

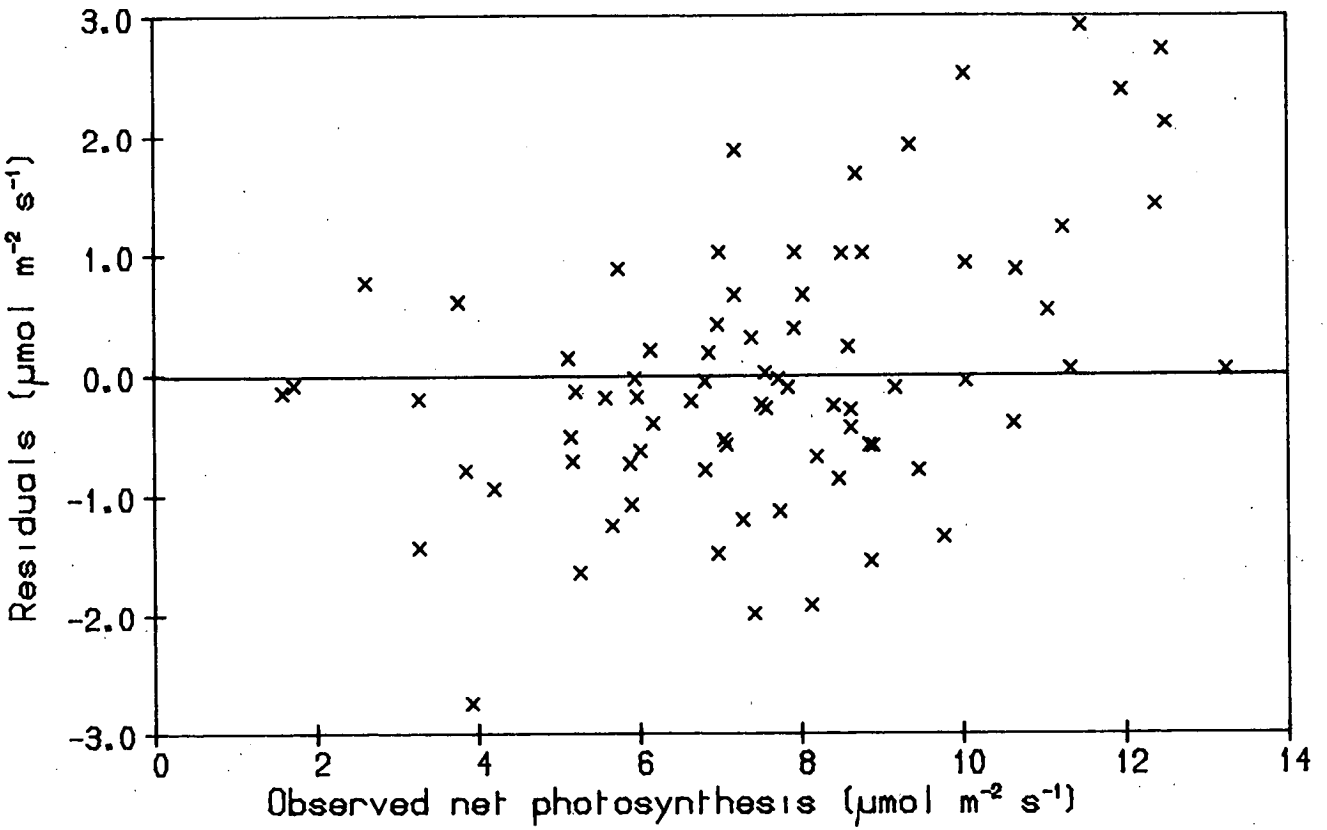

Fig. 5.5. Residual analysis of whorl 4 data fitted to function 5.7 with G and Rd fixed. Plot of net photosynthesis residuals (observed-predicted) against the dependent variable observed net photosynthesis.

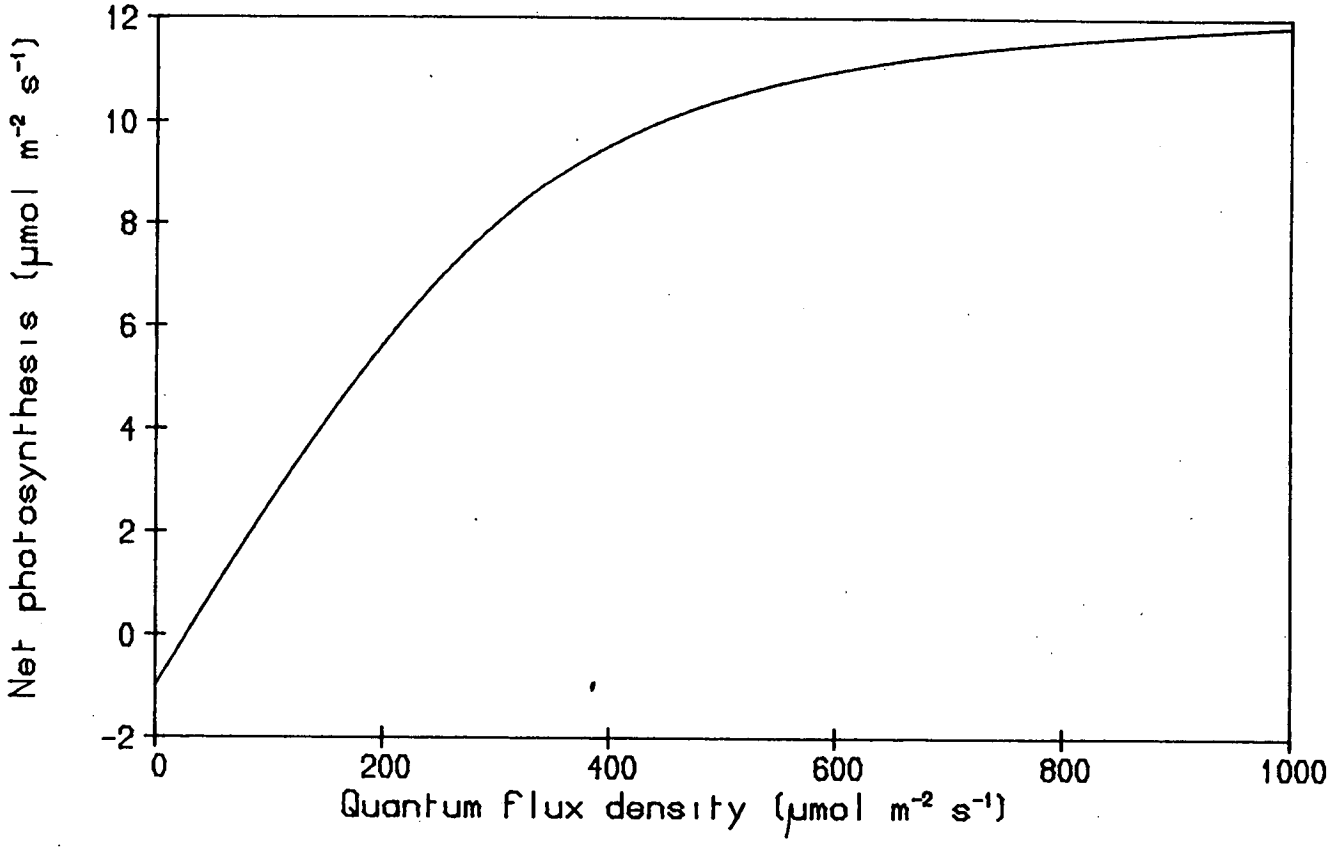

Fig. 5.6. Relationship between estimated net photosynthetic rate and quantum flux density for whorl 4 data, predicted using function 5.7 and derived parameters.

CHAPTER 6

RESULTS

The results from the four data sets were initially analysed individually and later considered together.

6.1 Terminal shoots on different whorls 1981

Table 6.1 shows the results of fitting function 5.7 to the 1981 current terminal shoot data summarised in table 6.2. The data set was divided up into three groups pertaining to the three different whorls investigated. In each case, the function was fitted to the data with the CO_2 compensation point fixed at a value of 50 μmol mol^{-1} to reduce the number of parameters to be estimated and thus avoid the estimation becoming unnecessarily complicated. Table 6.1 shows the results of the function fitted to the data with various combinations of the parameters M and R_d either fixed at a given value or estimated. It can be seen that for whorl 3, the mean square error (mse) was smallest without the values for M and R_d being fixed whereas for whorls 6 and 9, the mse was smallest when M was fixed at a value of 0.8. It is also obvious from table 6.1 that the regression coefficients for the fitted whorl 9 data, were low even though the corresponding mse values suggest a reasonable fit. This is because the regression coefficient depends just as much on the configuration of the data as on the success or otherwise of the function as an adequate description of the variation of the data (Ross, 1981). Table 6.2 shows that for whorl 9, the mean values of g_s, F_n and Q are all low compared to values for the other whorls, the low values being a direct result of shading due to canopy closure. This emphasises the need for an even spread of input

data values over a wide range to obtain a satisfactory description of response.

Table 6.2 also reveals that for all the whorls the minimum measured value of F_n was 0. In fact these values represent occasions when respiration exceeded photosynthesis. The function may have provided a better description of the data if these rates of net respiration had been known. However, Table 6.1 shows that for all whorls the mse was smallest when the value for R_d was low. This may be explained by the fact that the function was relatively insensitive to R_d as demonstrated by Fig. 5.4 previously.

The values estimated for a with data from whorls 3 and 6 were within the range expected and did not vary greatly when estimated using different combinations of fixed parameters. The values of a predicted with whorl 9 data varied to a larger extent with values ranging from 0.01 to 0.2.

The values estimated for g_m were also similar for whorls 3 and 6 and markedly lower for whorl 9. Table 6.2 shows that the mean stomatal conductances measured were correspondingly low for whorl 9 compared to whorls 3 and 6. It may be concluded that the photosynthetic responses of whorl 3 and 6 shoots to quantum flux density may not differ and that the apparent difference displayed by whorl 9 shoots may in part result from the distribution of the data as well as from physiological differences.

To compare the predicted responses of shoots between whorls within a data set and between different data sets, the function was fitted with M fixed at 0.8 and R_d fixed at 1.0 μmol m^{-2} s^{-1}. Fig. 6.1 shows the predicted response of net photosynthesis to quantum flux density, using the parameters shown in table 6.1 with set values for g_s, C_a and G of 0.12 mol m^{-2} s^{-1}, 320 μmol mol^{-1} and 50 μmol mol^{-1}, respectively.

As expected, there was little difference between whorls 3 and 6, but a large difference between the response predicted for whorl 9 as compared to whorls 3 and 6. The differences or similarities were investigated by combining the data from two whorls and fitting the function as before. Combining data from whorls 3 and 6, gave a mse of 4.57 which was smaller than previously obtained for whorl 3 alone but larger than had been obtained for whorl 6 alone. This suggested that there was in fact little difference between the predicted responses of the two whorls. Analysis of variance of the results of combined and individual fitted functions for whorls 3 and 6, produced a variance ratio of 0.2 which indicated that there was no discernible difference between them. Combining data from whorls 6 and 9 or whorls 3 and 9, revealed that the function fitted to the shoot data from whorl 9 was significantly different (P=0.001) from the functions fitted to whorls 3 and 6.

Table 6.1

Current terminal shoots 1981

N	M	R_d	a	gm	mse	n	r^2
3	0.8 *	1.0 *	0.0392	0.0586	5.740	81	46.6
6	0.8 *	1.0 *	0.0360	0.0626	3.379	73	56.9
9	0.8 *	1.0 *	0.01	0.0203	2.802	56	7.6
3	0.8 *	0.01	0.0307	0.0591	5.557	81	48.0
6	0.8 *	0.01	0.0281	0.0663	3.154	73	58.4
9	0.8 *	0.172	0.01	0.0084	2.381	56	9.5
3	0.0	1.0 *	0.0524	0.0770	5.492	81	48.3
6	0.0	1.0 *	0.0443	0.0906	3.283	73	56.7
9	0.976	1.0 *	0.20	0.0093	2.436	56	9.0
3	0.0	0.1	0.0392	0.0815	5.465	81	49.0
6	0.0	0.1	0.0319	0.1230	3.182	73	58.0
9	0.627	0.156	0.01	0.0101	2.426	56	10.0

N is the tree whorl number,

M is the convexity coefficient,

R_d is the rate of dark respiration (μmol m^{-2} s^{-1}),

a is the initial slope of the light response curve,

gm is the mesophyll conductance to CO_2 (mol m^{-2} s^{-1}),

mse is the mean square error of estimation,

n is the number of measurements used in estimation,

r^2 is the coefficient of multiple determination

* indicates a fixed parameter.

Table 6.2

Current terminal shoot (1981) data variables

N	V	mean	min	max
3	gs	0.209	0.028	0.432
3	Fn	5.442	0.000	15.585
3	T	14.85	2.90	25.50
3	Ca	319.12	305.00	331.00
3	Q	215.42	6.00	762.00
6	gs	0.206	0.096	0.417
6	Fn	4.278	0.000	12.887
6	T	14.33	5.34	22.30
6	Ca	317.72	308.00	326.00
6	Q	161.75	26.00	551.00
9	gs	0.160	0.001	0.534
9	Fn	0.612	0.000	9.559
9	T	12.43	4.30	20.00
9	Ca	318.94	310.00	340.00
9	Q	5.59	0.00	61.00

N is the tree whorl number,

V is the data variable:

gs is stomatal conductance to water vapour (mol m^{-2} s^{-1}),

Fn is the rate of net photosynthesis (μmol m^{-2} s^{-1}),

T is chamber air temperature (^{o}C),

Ca is ambient CO_2 concentration (μmol mol^{-1}),

Q is quantum flux density (μmol m^{-2} s^{-1}).

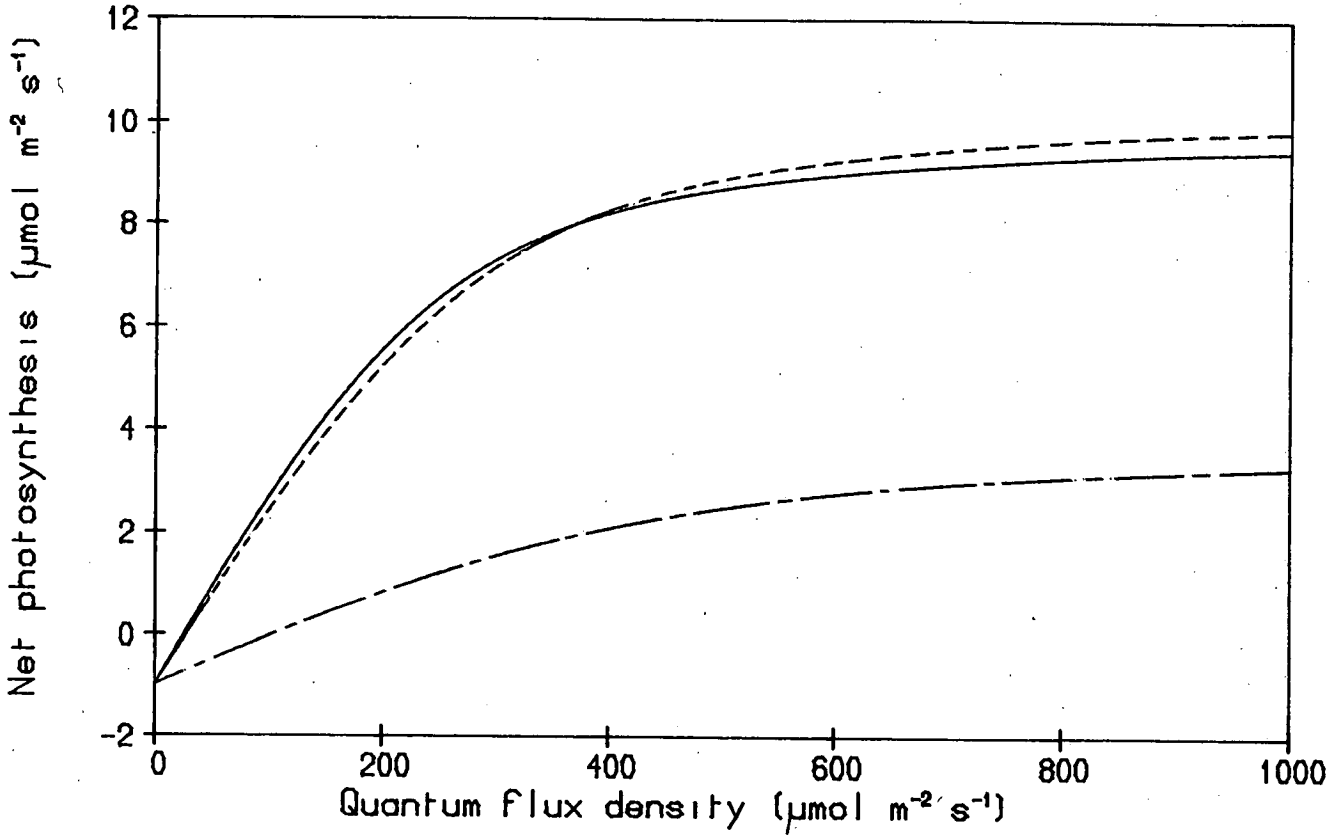

Fig. 6.1. Relationship between estimated net photosynthetic rate and quantum flux density for current year terminal shoots (1981), at whorl levels 3 (——), 6 (- - - -) and 9 (—— ——).

6.2 Developing shoots on the same whorl 1982

The data set was divided into two groups representing shoots with developing current year foliage and shoots without. The data were analysed in a similar way as before to give the results shown in table 6.3 derived from the data summarised in table 6.4. Both groups of shoots were on the same whorl of the same tree and hence experienced similar environmental conditions as shown in table 6.4. The mean values of g_s for both groups were also very similar but the mean F_n value for the shoots with developing foliage was less than half the value for the shoots with buds removed. For both groups of shoots the mse was smallest when R_d was fixed at a value of 1.0 μmol m^{-2} s^{-1}. When R_d was fixed, the estimated values for a were very similar for both groups while the estimated value of g_m for the shoots with buds removed was three times that of the developing shoots.

Fig. 6.2 shows the predicted response of net photosynthesis to quantum flux density, using the parameters estimated when M and R_d were fixed, together with the set values for g_s, C_a and G given before. As expected from the values of the parameters, the predicted rates of net photosynthesis were higher in the shoots with no developing foliage than the shoots with developing buds which appeared to become light-saturated at a lower quantum flux density. Combining the two groups of data and fitting the function with M and R_d fixed gave a mse of 4.67. Analysis of variance showed that there was highly significant difference (P=0.001) between the fitted functions for the two groups of data.

Table 6.3

Developing shoots 1982

S	M	R_d	a	gm	mse	n	r^2
R	0.8 *	1.0 *	0.0191	0.0390	5.718	95	28.0
D	0.8 *	1.0 *	0.0196	0.0138	2.296	100	14.7
R	0.8 *	0.1	0.0125	0.0395	5.496	95	30.1
D	0.8 *	0.1	0.0084	0.0483	2.254	100	15.8
R	0.0	1.0 *	0.0259	0.0483	5.470	95	30.3
D	0.0	1.0 *	0.0301	0.0158	2.253	100	15.9
R	0.0	3.0	0.0646	0.0484	5.632	95	28.1
D	0.0	0.21	0.0129	0.0138	2.260	100	16.4

S is the type of shoot: R (bud removed), D (developing bud),

M is the convexity coefficient,

R_d is the rate of dark respiration (μmol m^{-2} s^{-1}),

a is the initial slope of the light response curve,

gm is the mesophyll conductance to CO_2 (mol m^{-2} s^{-1}),

mse is the mean square error of estimation,

n is the number of measurements used in estimation,

r^2 is the coefficient of multiple determination

* indicates a fixed parameter.

Table 6.4

Developing shoot (1982) data variables

S	V	mean	min	max
R	gs	0.087	0.008	0.165
R	Fn	2.909	0.250	14.030
R	T	23.41	13.80	30.60
R	Ca	324.28	317.00	345.00
R	Q	349.37	49.00	1439.00
D	gs	0.079	0.003	0.394
D	Fn	1.350	0.080	7.730
D	T	23.18	14.00	31.40
D	Ca	323.00	316.00	339.00
D	Q	388.64	29.00	1683.00

S is the type of shoot: R (bud.removed), D (bud developing),

V is the data variable:

gs is stomatal conductance to water vapour (mol m^{-2} s^{-1}),

Fn is the rate of net photosynthesis (μmol m^{-2} s^{-1}),

T is chamber air temperature (^{o}C),

Ca is ambient CO_2 concentration (μmol mol^{-1}),

Q is quantum flux density (μmol m^{-2} s^{-1}).

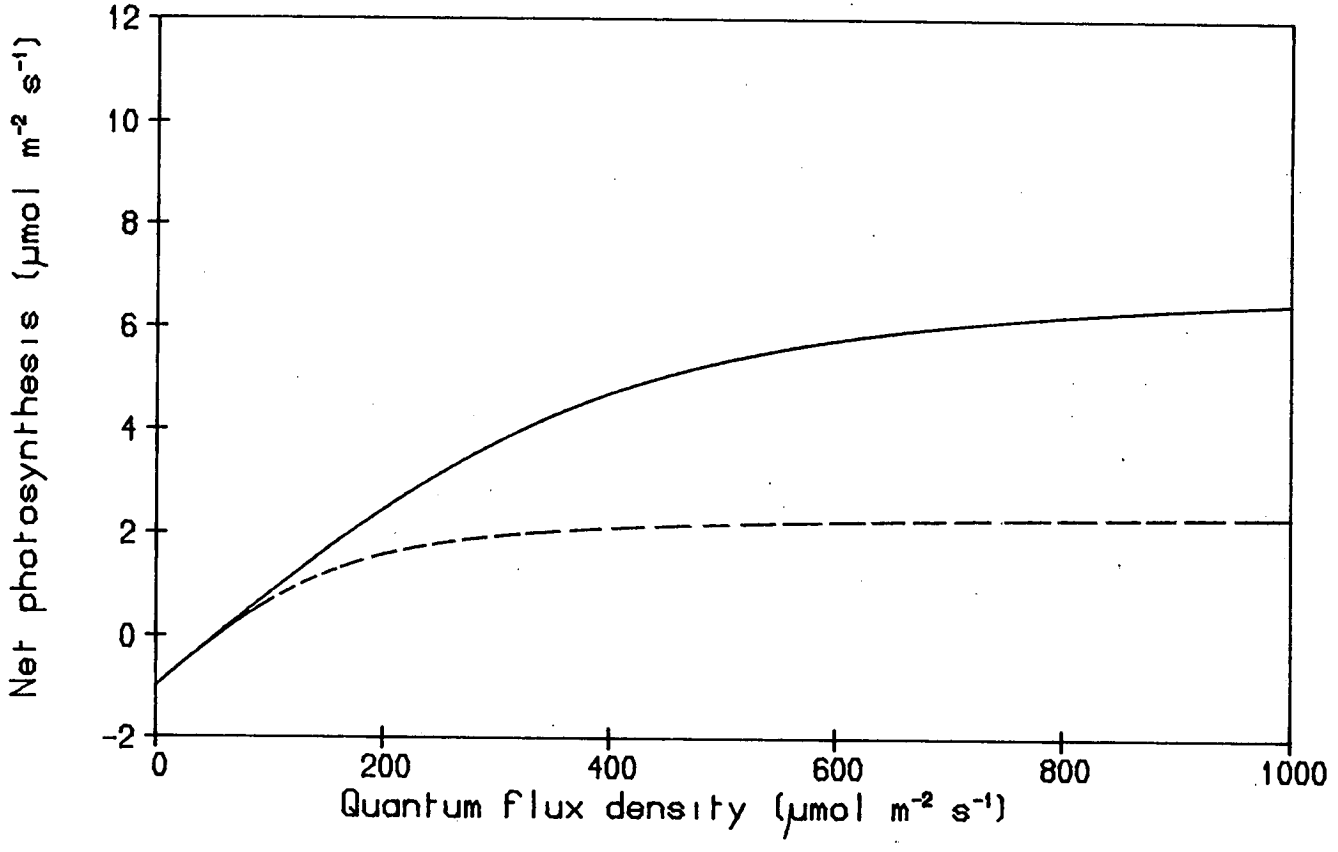

Fig. 6.2. Relationship between estimated net photosynthetic rate and quantum flux density for one-year-old shoots with developing 1982 foliage (- - -) and for shoots with developing foliage removed (———).

6.3 Terminal shoots on different whorls 1982

Table 6.5 shows the results of fitting function 5.7 to current terminal shoot data summarised in table 6.6. Results are shown from measurements made on whorls 3, 4 and 5. Table 6.6 shows that the mean values for g_s, T and C_a were all very similar irrespective of whorl number. On the other hand the mean values of Q became lower further down into the canopy as might be expected. The mean values for F_n were similar for whorls 3 and 4 but much lower for whorl 5. Table 6.5 shows that for all three whorls investigated the mse was smallest when R_d was fixed at a value of 1.0 μmol m^{-2} s^{-1}. It can also be seen that in all cases the mse values corresponded well with the r^2 values, suggesting that the data were evenly spread over their range. The estimated values of a and g_m for whorls 3 and 4 did not appear to differ greatly but were consistently different from the values estimated for whorl 5. The value for a was larger and the value for g_m was smaller for whorl 5 shoots than was estimated for shoots from whorls 3 and 4.

Fig. 6.3 shows the predicted response of net photosynthesis to quantum flux density using the parameters estimated when M and R_d were fixed as before. There appeared to be little difference between the responses of whorls 3 and 4 although the predicted response of whorl 4 had a slightly steeper initial slope (a) and a higher asymptote. The response predicted for whorl 5 was as expected from the parameter estimates in table 6.5: the initial slope was steeper, photosynthesis became light-saturated at a lower quantum flux density and photosynthesis reached a lower asymptote than for the other whorls. Combining the data from whorls 3 and 4 and fitting the function as before resulted in a mse of 1.59 which was not significantly lower

than the values obtained when the function was fitted to the whorl data individually. Combining data from whorls 4 and 5 or whorls 3 and 5 resulted in mse values of 2.24 and 2.45, respectively. This suggested that the response curve of whorl 5 might indeed be different from that of the other two whorls. Analysis of variance revealed that although the difference between the responses of whorls 3 and 4 was not particuarly significant (P=0.05), the differences between whorls 3 and 5 and also between whorls 4 and 5, were in fact highly significant (P=0.001).

Table 6.5

Current terminal shoots 1982

N	M	R_d	a	gm	mse	n	r^2
3	0.8 *	1.0 *	0.0308	0.0800	1.639	80	76.7
4	0.8 *	1.0 *	0.0369	0.0831	1.422	79	79.0
5	0.8 *	1.0 *	0.0627	0.0474	2.303	78	57.3
3	0.8 *	2.637	0.0407	0.0894	1.616	80	76.9
4	0.8 *	0.100	0.0309	0.0781	1.398	79	79.4
5	0.8 *	0.425	0.0525	0.0454	2.318	78	57.8
3	0.387	1.0 *	0.0365	0.0942	1.612	80	77.8
4	0.054	1.0 *	0.0511	0.0999	1.252	79	81.7
5	0.0	1.0 *	0.0875	0.0583	2.094	78	61.5
3	0.0	2.002	0.0547	0.1000	1.566	80	79.4
4	0.0	1.302	0.0532	0.1059	1.258	79	81.7
5	0.0	1.297	0.0962	0.0594	2.119	78	60.5

N is the tree whorl number,

M is the convexity coefficient,

R_d is the rate of dark respiration (μmol m^{-2} s^{-1}),

a is the initial slope of the light response curve,

gm is the mesophyll conductance to CO_2 (mol m^{-2} s^{-1}),

mse is the mean square error of estimation,

n is the number of measurements used in estimation,

r^2 is the coefficient of multiple determination

* indicates a fixed parameter.

Table 6.6

Current terminal shoot (1982) data variables

N	V	mean	min	max
3	gs	0.128	0.078	0.246
3	Fn	8.060	1.330	13.140
3	T	25.22	17.70	30.20
3	Ca	315.95	305.00	337.00
3	Q	610.71	85.00	1318.00
4	gs	0.118	0.054	0.285
4	Fn	7.493	1.580	13.240
4	T	26.04	17.70	31.90
4	Ca	314.44	305.00	332.00
4	Q	478.21	59.00	1152.00
5	gs	0.117	0.038	0.367
5	Fn	4.278	0.330	11.400
5	T	25.19	17.90	29.70
5	Ca	314.26	305.00	330.00
5	Q	182.68	4.00	1066.00

N is the tree whorl number,

V is the data variable:

gs is stomatal conductance to water vapour (mol m^{-2} s^{-1}),

Fn is net rate of photosynthesis (μmol m^{-2} s^{-1}),

T is chamber air temperature (^{o}C),

Ca is ambient CO_2 concentration (μmol mol^{-1}),

Q is quantum flux density (μmol m^{-2} s^{-1}).

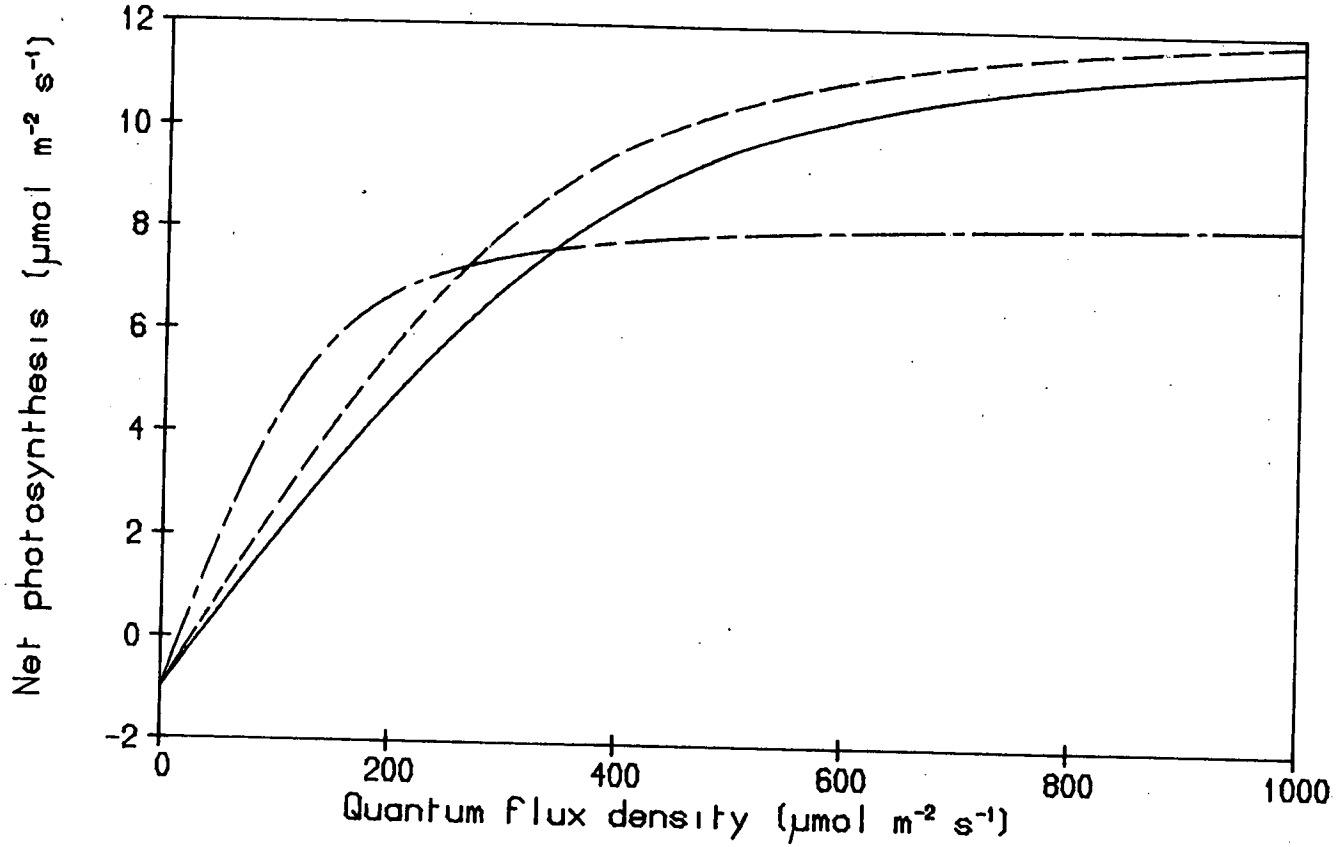

Fig. 6.3. Relationship between estimated net photosynthetic rate and quantum flux density for current year terminal shoots (1982), at whorl levels 3 (——), 4 (- - -) and 5 (-·——).

6.4 One-year-old lateral shoots on different whorls 1982

This set of data was measured on the same whorl branches on the same trees as in the previous section but was different in that the shoots measured were lateral shoots that had developed in the previous year (1981). Table 6.7 shows the results of fitting the function to the data as before, using the data in table 6.8. As with the terminal shoots (table 6.6), the mean values for g_s, T and C_a were similar for all three whorls investigated. The mean values for F_n and Q were lower further into the canopy and were also lower than the mean values obtained for current shoots previously.

Table 6.7 shows that for all three whorls the mse was smallest when there were no constraints on the parameters. Under these conditions the values obtained for M and R_d were both very small. The mse was larger and the r^2 small for whorl 3 data suggesting a poor fit. The estimated values for a were similar for whorls 3 and 4 but the estimated value for g_m was consistently higher in whorl 4 shoots. Whorl 5 shoots appeared to have a higher value for a than the other whorl shoots and a value of g_m similar to that predicted for whorl 3 shoots.

Fig. 6.4 shows the predicted responses of lateral shoots from the three whorls as described previously. The predicted response for whorl 5 shoots had a steeper initial slope and reached an asymptote at a lower quantum flux density. As with the terminal shoots in the previous section, the predicted response of whorl 4 shoots displayed a steeper initial slope and higher asymptote than the response of whorl 3 shoots, the difference being more pronounced in this case. The asymptotic value predicted for whorl 3 shoots was not much higher than the value predicted for whorl 5 shoots. Combining data from whorls 3

and 5 and fitting the function produced a mse value of 4.42 which indicated that there was in fact a significant difference between whorl 3 and whorl 5 shoots. Similarly combining data from whorls 3 and 4 or 4 and 5, resulted in mse values of 4.39 and 2.35, respectively. Analysis of variance showed that the most significant difference was between the shoots of whorls 4 and 5 (P=0.001). The differences between whorl 3 and 4 shoots (P=0.01) and between whorl 3 and 5 shoots (P=0.05), were also significant but at a lower level of probability.

Table 6.7

One year old lateral shoots 1982

N	M	R_d	a	gm	mse	n	r^2
3	0.8 *	1.0 *	0.0425	0.0496	3.918	73	24.1
4	0.8 *	1.0 *	0.0468	0.0706	2.339	69	71.6
5	0.8 *	1.0 *	0.0761	0.0367	2.005	55	51.6
3	0.8 *	0.1	0.0344	0.0456	3.723	73	25.1
4	0.8 *	0.1	0.0368	0.0713	2.115	69	73.6
5	0.8 *	0.1	0.0493	0.0408	1.832	55	55.4
3	0.0	1.0 *	0.0624	0.0605	3.810	73	23.9
4	0.0	1.0 *	0.0610	0.0926	2.139	69	73.3
4	0.0	1.0 *	0.0935	0.0533	1.876	55	54.2
3	0.0	0.1	0.0489	0.0568	3.668	73	24.8
4	0.097	0.1	0.0454	0.0941	2.096	69	74.0
5	0.0	0.1	0.0577	0.0662	1.757	55	57.0

N is the tree whorl number,

M is the convexity coefficient,

R_d is the rate of dark respiration (μmol m^{-2} s^{-1}),

a is the initial slope of the light response curve,

gm is the mesophyll conductance to CO_2 (mol m^{-2} s^{-1}),

mse is the mean square error of estimation,

n is the number of measurements used in estimation,

r^2 is the coefficient of multiple determination

* indicates a fixed parameter.

Table 6.8

One year old shoot (1982) data variables

N	V	mean	min	max
3	gs	0.162	0.034	0.815
3	Fn	5.782	1.120	11.330
3	T	15.90	9.60	21.10
3	Ca	321.29	307.00	337.00
3	Q	330.64	27.00	1518.00
4	gs	0.119	0.020	0.396
4	Fn	4.934	0.250	12.350
4	T	16.29	11.40	21.60
4	Ca	319.39	306.00	331.00
4	Q	198.41	6.00	857.00
5	gs	0.122	0.058	0.350
5	Fn	3.387	0.580	8.030
5	T	15.48	10.70	20.00
5	Ca	319.14	306.00	330.00
5	Q	82.73	13.00	235.00

N is the tree whorl number,

V is the data variable:

gs is stomatal conductance to water vapour (mol m^{-2} s^{-1}),

Fn is the rate of net photosynthesis (μmol m^{-2} s^{-1}),

T is chamber air temperature (^{o}C),

Ca is ambient CO_2 concentration (μmol mol^{-1}),

Q is quantum flux density (μmol m^{-2} s^{-1})

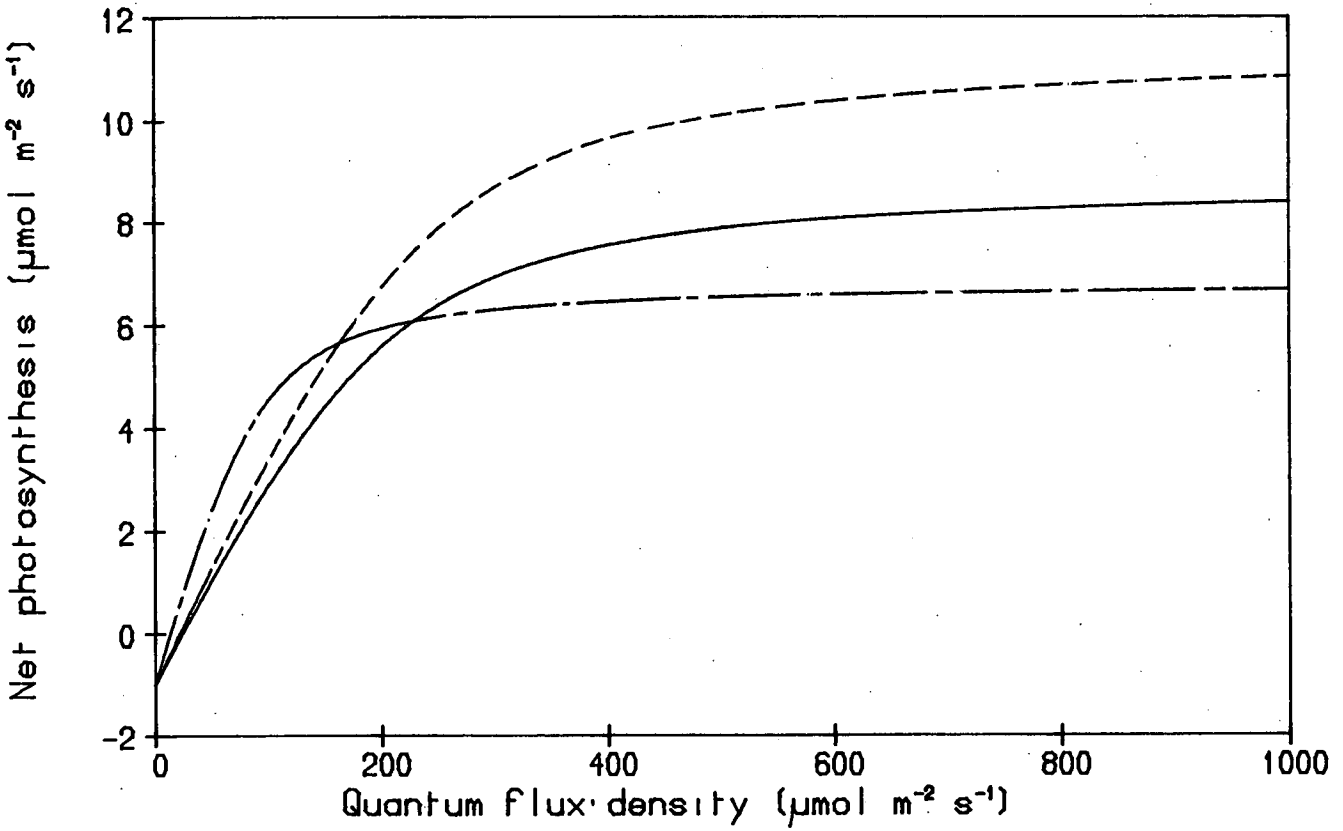

Fig. 6.4. Relationship between estimated net photosynthetic rate and quantum flux density for one-year-old lateral shoots (1982), at whorl levels 3 (——), 4 (- - -) and 5 (-·—).

6.5 Current and one-year-old shoots on the same whorl

The data discussed in sections 6.3 and 6.4 were measured on the same whorls of the same trees within the same month. The two data sets differed in that the shoots measured were of different ages and were either lateral or terminal shoots. The effects of needle age combined with shoot position, could therefore be investigated by comparing the two sets of data. Tables 6.5 and 6.7 reveal that when M and R_d were fixed the estimated values for a were higher and the values for g_m were lower in lateral shoots than in terminal shoots for all three whorls. Fig. 6.5 shows the predicted responses of current terminal and one-year-old lateral shoots from whorl 3. The one-year-old response curve appears to be steeper initially and have a lower asymptote than that for the current terminal shoots. Combining the whorl 3 data from both sets and fitting function 5.7, resulted in a mse of 3.99. Fig. 6.6 shows the responses of the two different types of whorl 4 shoots. There appears to be much less difference between the responses but again the initial slope of the one year old shoots was steeper and the asymptote slightly lower. Fitting the function to the combined data sets gave a mse value of 1.89. Fig. 6.7 depicts the responses of whorl 5 shoots of the two types measured. There appeared to be only a slight difference in the initial slopes but the predicted asymptote for one year old shoots was lower. Fitting the function to the combined data as before gave a mse value of 2.18. Analysis of variance of the predicted fitted functions suggested that the differences between the two groups of shoots were highly significant for whorls 3 ($P=0.01$) and 4 ($P=0.001$) but not so significant for whorl 5 ($P>0.2$).

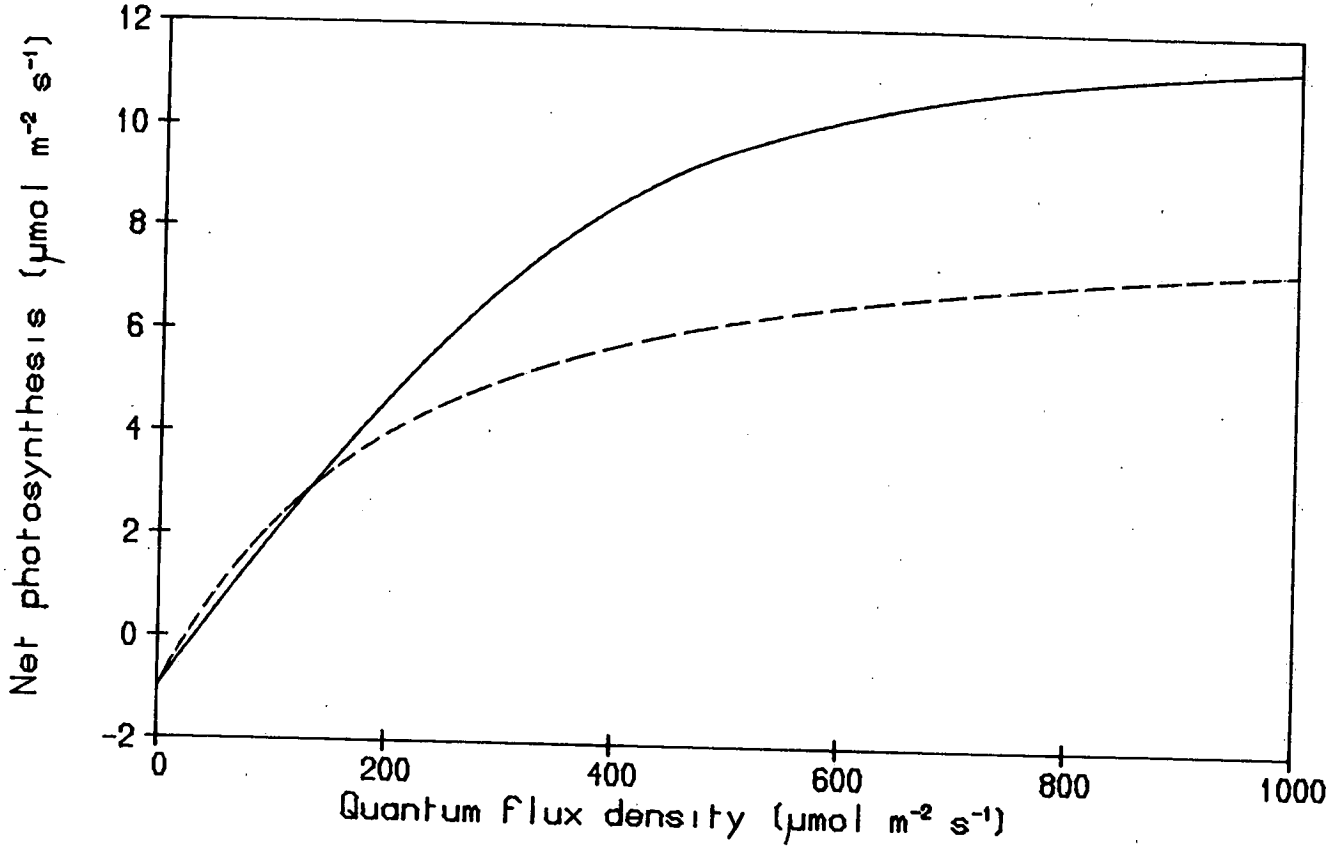

Fig. 6.5. Relationship between estimated net photosynthetic rate and quantum flux density for 1982 current terminal shoots from whorl 3 (——) and one-year-old lateral shoots from whorl 3, measured in 1982 (- - -).

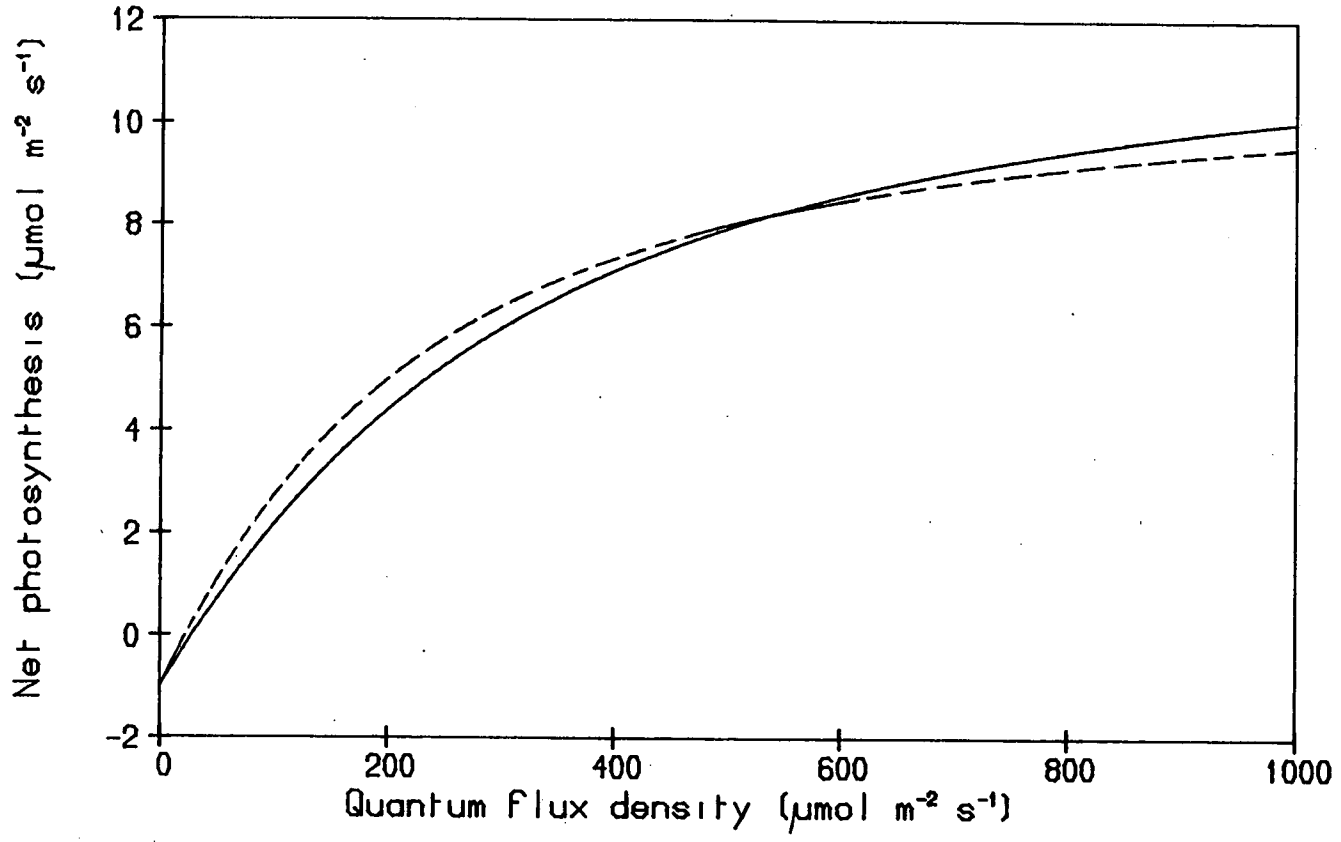

Fig. 6.6. Relationship between estimated net photosynthetic rate and quantum flux density for 1982 current terminal shoots from whorl 4 (——) and one-year-old lateral shoots from whorl 4, measured in 1982 (- - -).

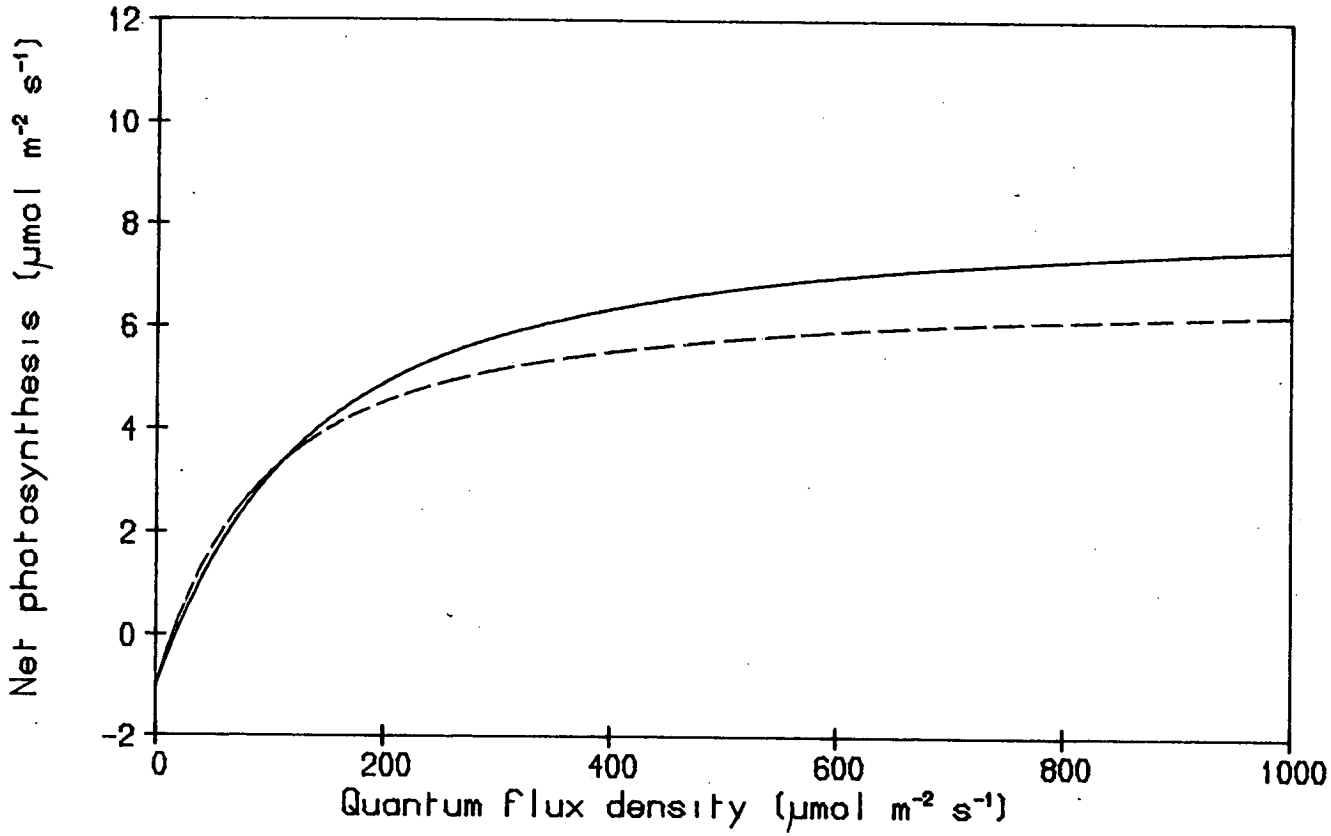

Fig. 6.7. Relationship between estimated net photosynthetic rate and quantum flux density for 1982 current terminal shoots from whorl 5 (——) and one-year-old lateral shoots from whorl 5, measured in 1982 (– – –).

6.6 Shoots on whorl 3 1981-2

Current year terminal shoots on whorl 3 were measured both in 1981 and in 1982. Tables 6.1 and 6.5 reveal that when M and R_d were fixed the estimated values for a were similar for both years and the value for g_m in 1982 was higher than value estimated using 1981 data. Comparing tables 6.2. and 6.6 shows that during the period of measurement in 1981, the mean values for temperature and quantum flux density were much lower than the period of measurement in 1982. Measurements were made during August to October in 1981 whereas 1982 measurements were made during July. The mean values for F_n were lower and the mean values for g_s were higher in 1981 compared to 1982, which may be a direct result of the environmental conditions. Different trees were measured in each year but they were all of the same intermediate social status.

Fig 6.8 shows the predicted responses of whorl 3 terminal shoots measured in 1981 and 1982. The predicted responses of the two groups of shoots did not differ greatly. The 1981 shoots had a steeper initial slope and reached a lower asymptote at a lower quantum flux density. Combining whorl 3 data from both years and fitting the function produced a mse value of 3.79 which indicated that there was in fact little difference between the predicted responses for both years. Analysis of variance showed the difference not to be particuarly significant (P=0.05).

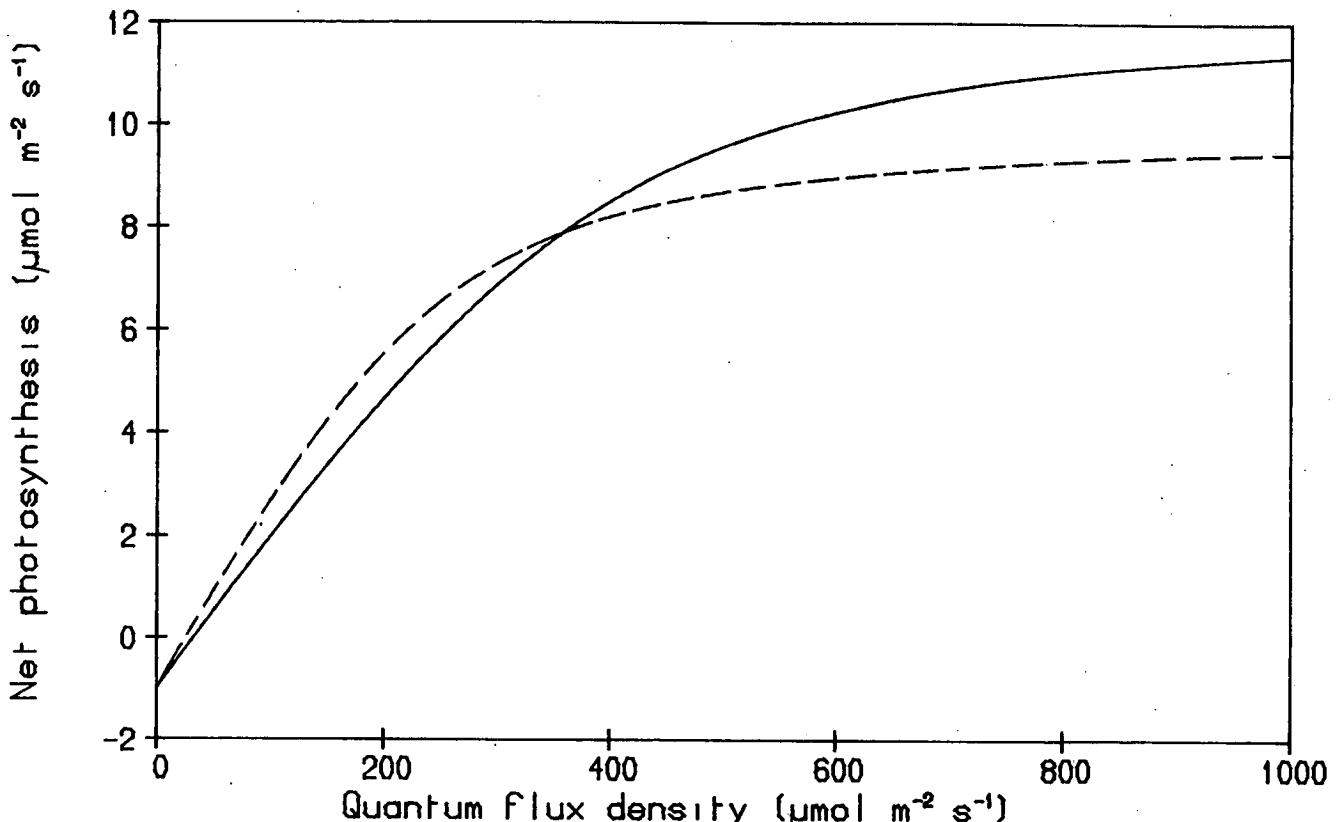

Fig. 6.8. Relationship between estimated net photosynthetic rate and quantum flux density for current terminal shoots from whorl 3 measured in 1981 (- - -) and 1982 (———).

CHAPTER 7

DISCUSSION

7.1 Equipment and fieldwork

The equipment performed well under field conditions and there were no major problems regarding the design and operation. Once at the site the equipment could be set up and be operational within 15 minutes. Measurements of stomatal conductance and net photosynthesis together took between three and five minutes and a normal sample run of twelve shoots could be measured within an hour. If another pair of operators had been available there would have been no practical reason why measurements could not have been made continuously throughout daylight hours allowing up to 150 measurements to be made.

An initial problem was access to the upper parts of the canopy, because the trees had outgrown the scaffolding which had been constucted some years ago. The structure was extended with extra steelwork and a section of portable aluminium scaffolding. The modified structure allowed access to the majority of the canopy but chamber operators still had to stretch to reach some shoots. This limitation was taken into consideration when selecting shoots for measurements. In an ideal situation the scaffolding should not interfere with the surrounding trees but inevitably there was some shading and mechanical damage to the trunks of trees. The trees selected for investigation were, as far as possible, free from mechanical damage and excessive shading from the scaffolding.

The major problem encountered was that of weather. The Greskine forest is situated in an area that has an above average mean annual rainfall for the U.K. Measurements of stomatal conductance could not

be carried out on wet foliage since surface water would have caused an overestimation of transpiration. Measurements of net photosynthesis may also have been affected by the physical presence of water interfering with CO_2 transfer or by water vapour affecting the measurement of CO_2 concentration. Often early morning dew or mist delayed measurements until the foliage was deemed dry enough for investigation to begin. A light shower of rain could hold up measurements for a number of hours especially if the lower canopy became wet.

7.2 Sampling strategy

Measurements were usually made over a number of days but inevitably the spread of data with respect to environmental variables, such as quantum flux density, was not ideal. In particular the shoots measured lower down in the canopy rarely experienced high quantum flux densities during measurements. This may be natural but it is important to have such measurements at high quantum flux densities to be able to compare with confidence the response of net photosynthesis with that of shoots further up the canopy. One solution would have been to supplement the quantum flux density at lower levels with an artificial light source but this condition is far from natural. A simple answer that was implemented where possible was to pull back any branches above that may have caused shading. The other main variable that was used in the eventual fitting of the function to the data was stomatal conductance to CO_2. This was derived from measurements of stomatal conductance to water vapour. Stomatal conductance is strongly correlated with quantum flux density in the absence of other limiting factors such as vapour pressure deficit. Thus values for stomatal

conductance tend to be high at high quantum flux densities. Consequently the measurents tend to be biased with values lacking at high quantum flux density and low stomatal conductance or low quantum flux density and high stomatal conductance. This undoubtedly affects the goodness of fit of the function used for data analysis.

Measurements were taken throughout the day from early morning to late evening where possible. No account was taken of endogenous trends in the analysis of the measurements. It was assumed that any variation resulting from endogenous trends would be similar for the different populations of shoots measured.

The longest period spent measuring one population of shoots was in 1981 when measurements were carried out over a period of two months in late autumn. For analysis it was assumed that the photosynthetic responses might not vary so much over this period as they would during spring, so the data were analysed as one homogenous set.

With the exception of the growing shoot experiments, it was assumed that the shoot needle area would not increase significantly over the measuring period. Some needles may have been lost as a result of placing the shoot in the chamber but these losses were considered to be a small proportion of the total shoot area. In the case of the growing shoots, shoots that were similar in size and development were removed and the leaf areas measured.

Analysis of the F_n and g_s measurements showed that most of the variation between replicates was amongst the different shoots within a tree as opposed to between the different trees. Values for F_n and g_s measured within trees had standard deviations of about 25% the mean values. However, a large amount of the variation in F_n and g_s observed may be accounted for by the variation in quantum flux densities which had standard deviations of 45% the mean values. This highlights the

problems encountered with many gas exchange studies in which assimilation chambers are used on small numbers of shoots for intensive investigations. The shoots measured may not be representative of the population and consequently erroneous conclusions may be drawn. To take account of the variability encountered between shoots within the same population, it is therefore desirable to carry out an extensive investigation of the canopy in the first instance.

In a number of cases, particularly in the lower whorls, quantum flux density was so low that net respiration occurred. It would have been desirable to measure this but this was not considered practical at the time since it would have involved changing air supplies and flushing the whole porometer system with the new gas for at least ten minutes.

7.3 Data handling

Mathematical functions were used to describe the data and take into account the influences of particular variables. The efficiency with which a particular function describes data or takes into account variability was expressed in terms of mse or r^2. The errors involved consist of two distinct components, the error associated with measurement and the error due to the inadequacy of the model in representing the situation. The mean square error takes into account both errors whereas the r^2 value is a comparison of predicted rate against observed rate and does not take into account the variability of the data. Table 6.5 shows the mse and r^2 values to agree well but table 6.1 demonstrates a lack of agreement particularly for shoots from whorl 9. The mse suggests a good fit to the data whereas the r^2 value indicates that the predicted rates of net photosynthesis are

different from those observed. Further analysis of the data for whorl 9 revealed poor distribution of the data with respect to quantum flux density, indicating that the predicted parameters are in fact a good description of unevenly spread data.

In some cases the data were not adequate enough to predict confidently all the parameters of function 5.7, so the number of parameters was reduced by assigning fixed values to those that could not be predicted accurately. For the sake of comparison these parameter were fixed at the same value for all the populations compared. The consequence of this may have been greater in some cases than others. Dark respiration rate was one of the fixed parameters and may have influenced the estimated value of a to a greater extent in shoots that had low net photosynthetic rates as compared to shoots with high rates of net photosynthesis.

The validation carried out suggested that the function was indeed a good description of the data and accounted for much of the variability. It was therefore considered a useful tool with which to analyse field data and to predict rates of net photosynthesis for the canopy.

7.4 Source of variation

To attach any biological significance to the differences observed between shoots in Chapter 6, it is necessary to be able to identify the sources of variation. Differences between populations of shoots may result from a number of variables including error in measurement, inadequacy of the function in describing the data, variation within the sample and also actual differences between populations. There will be a certain amount of error in the measured data which is attributable to the measuring technique used. For example, there may

be human bias in balancing for stomatal conductance and net photosynthesis or calibration errors associated with the instruments used. The equipment and measuring technique were designed to minimise any errors that may occur. However, larger errors are likely to occur when stomatal conductance and rates of net photosynthesis are small. Environmental conditions may also affect the performance of the instruments as shown previously in Chapter 3, when considering temperature differences within the chamber.

The second source of error mentioned, inadequacy of the function, relates to the technique used to interpret the shoot data. The function used may not be adequate to describe the response of all different types of shoots and there is some evidence of this as skewness in the residual analysis. Some of this error may be a result of the uneven spread of data for some populations of shoots. The data were not considered good enough to be able to predict all the parameters of the function anyway and a more complex model does not seem justified from the field data.

The third source of variation may be within a population of shoots. Analysis of the data for individual shoots at a particular whorl revealed that variation was larger amongst shoots from the same tree than between mean values for trees. A number of replicates on each tree were sampled to reduce this source of variation.

The final source of variation is a real difference between shoot populations - the difference that was to be considered at the outset of the investigation. There may indeed be differences but these must be considered in the light of the previous discussion.

7.5 Biological implications

Measurements made on different whorls on different aged shoots

suggest that there are differences between the photosynthetic properties of the shoots. In all cases the predicted rates of net photosynthesis at a particular quantum flux density were lowest for the shoots that were deepest into the canopy. This difference is probably a response to the environment in which the shoots developed and grew. The quantum flux densities are substantially lower further into the canopy and the shoots growing there should exhibit acclimation to shade. This was greatest in the shoots measured in 1981 on whorl 9: these had a lower predicted rate of net photosynthesis over the whole range of quantum flux densities than the shoots at whorls 3 and 4. The results from current and one-year-old shoots measured in 1982 showed smaller differences between whorls 3, 4 and 5 but whorl 9 was not measured. Shoots at the lowest whorl had a lower predicted asymptotic rate of net photosynthesis but higher initial slope at lower quantum flux densities than was displayed by shoots from higher whorls. This is a typical response of shade-acclimated foliage but may be partly a consequence of fixing the values for R_d and M in fitting the function. The differences between the whorl 3 and 4 shoots was small but it is noteworthy that for both current and one-year-old shoots 1982, the predicted rates of net photosynthesis were higher for shoots at whorl 4 than at whorl 3 at the same quantum flux density. The whorl 4 shoots recieved slightly lower quantum flux densities than whorl 3 shoots since they were positioned at the level of the beginning of canopy closure.

The shoots with expanding foliage at the time of measurement had lower predicted rates of net photosynthesis than shoots with the developing foliage removed. This is as might be expected since it has been shown in the field (Troeng and Linder 1981) that developing shoots are net importers of carbon imediately after bud break and have

a high respiration rate associated with growth. It might have been more useful to study the responses of developing foliage and its supportive previous year shoots separately, since it is to be expected that the supporting shoots would be more active than shoots without buds, because of demands of the developing shoots for assimilate.

The differences between current and one-year-old shoots in response to quantum flux density were not great but one-year-old shoots were consistently predicted as having lower asymptotic rates of net photosynthesis and slightly higher initial slopes. The largest difference predicted was between the different shoots from whorl 3 in 1982. However the fit of the function for one-year-old shoots from whorl 3 was not particularly good and too much importance should not be assigned to this observation.

To conclude, the investigation shows that the differences in response of current and one-year-old shoots to quantum flux density were small above the level of canopy closure. Parameters of a single fit of the function to all these shoots might provide a reasonable description of the data. The shoots below the level of canopy closure exhibited larger differences in response to quantum flux density and warrant further investigation. Future studies of net photosynthesis within the canopy should include measurements of respiration of shoots throughout the canopy. Sufficient data should also be collected throughout a range of quantum flux densities and at various stomatal conductances since it has been shown how important the distribution of the data is on the fitting to the function.

Clearly the measuring technique developed has many advantages over previous methods and could be used for similar and more intensive studies than that described on the same or other species of plants.

REFERENCES

BEADLE, C.L., TURNER, N.C., and JARVIS, P.G., 1978. Critical water potential for stomatal closure in Sitka spruce. Physiologia Pl. 43, 160-165.

BEADLE, C.L., JARVIS, P.G., and NEILSON, R.E., 1979. Leaf conductance as related to xylem water potential and carbon dioxide concentration in Sitka spruce. Physiologia Pl. 45, 158-166.

BEARDSELL, M.F., JARVIS, P.G., and DAVIDSON, B., 1972. A null-balance diffusion porometer suitable for use with leaves of many shapes J.A.Ecol. 9, 667-90.

BELL, C.J., and INCOLL, L.D., 1981. A handpiece for the simultaneous measurement of photosynthetic rate and leaf diffusive conductance J.exp.Bot. 32, 1125- 1134.

BMDP, PAR. Derivative-free nonlinear regression package. In BMDP Statistical Software 1981. Department of Biomathematics, University of California, Los Angeles. University of California Press. 305-314.

BRAVDO, B.A., 1972. Photosynthesis, transpiration, leaf stomatal and mesophyll resistance measurements by use of a ventilated diffusion porometer. Physiologia Pl. 27, 209-15.

COCHRANE, L.A., and FORD, E.D., 1978. Growth of a Sitka spruce plantation: Analysis and stochastic description of the development of the branching structure. J. A. Ecol. 15, 227-244.

de WIT, C.T., 1965. Photosynthesis of leaf canopies. Agric. Res. Dept. No. 663. Centre of Agric. Publ., and Doc., Wageningen.

EHLERINGER, J., and COOK, C.S., 1980. Measurements of photosynthesis in the field: utility of the CO_2 depletion technique. Plant, Cell and Enviroment. 3, 479-482.

FANJUL, L., JONES, H.G., and TREHARNE, K.J., 1980. A portable system for simultaneous measurement of transpiration and CO_2 exchange. Photosynth. Res. 1, 83-92.

FORD, E.D., and DEANS, J.D., 1977. Growth of a Sitka spruce plantation: spatial distribution and seasonal fluctuations of lengths, weights and carbohydrate concentrations of fine roots. Plant and Soil 47, 463-485.

FORD, E.D., and DEANS, J.D., 1978. The effects of canopy structure on stemflow, throughfall and interception loss in a young Sitka spruce plantation. J. A. Ecol. 15, 907-917.

FORD, E.D., 1982. High productivity in a pole stage Sitka spruce stand and its relation to canopy structure. Forestry 55, 1-17.

GOUDRIAAN, J., 1978. A family of saturation type curves, especially in relation to photosynthesis. Ann. Bot. 43, 783-785.

JARVIS, P.G., 1971. The estimation of resistances to carbon dioxide transfer. In Plant Photosynthetic Production: Manual of Methods. Eds. Z.Sestak, J.Catsky, and P.G.Jarvis. Dr.W.Junk, N.V., The Hague. Pp. 566-631.

JARVIS, P.G., 1981. Production efficiency of coniferous forests in the U.K. In phsiological processes limiting plant productivity. Ed. JOHNSON, C.B., (Butterworths). 5, 81-107.

JOHNSON, H.P., ROWLANDS, P.G., and TING, I.P., 1979. Tritium and carbon-14 double isotope porometer for simultaneous measurements of transpiration and photosynthesis. Photosynthetica, 12, 409-18.

KOLLER, D., and SAMISH, Y., 1964. A null-point compensating system for simultaneous and continuous measurement of net photosynthesis and transpiration by controlled gas-stream analysis. Bot. Gaz. 125, 81-8.

LEVERENZ, J.W., DEANS, J.D., FORD, E.D., JARVIS, P.G., MILNE, R., and WHITEHEAD, D., 1982. Systematic spatial variation of stomatal conductance in a Sitka spruce plantation. J. A. Ecol. 19, 835-851.

LEVERENZ, J.W., and JARVIS, P.G., 1979. Photosynthesis in Sitka spruce (Picea sitchensis (Bong.) Carr.) VIII. The effects of light flux density and the direction on the rate of net photosynthesis and the stomatal conductance of needles. J. A. Ecol. 16, 919-932.

LEVERENZ, J.W.,and JARVIS, P.G., 1979. Photosynthesis in Sitka spruce (Picea sitchensis (Bong.) Carr.) IX. The relative contribution made by needles at various positions on the shoot. J. A. Ecol. 17, 59-68.

LEVERENZ, J.W., 1979. Convexity and net quantum efficiency of the light response curve of photosynthesis. Swedish Coniferous Forest Project. Technical report 25.

LEVERENZ, J.W., 1981. Photosynthesis and transpiration in a large forest-grown Douglas fir: Diurnal variation. Can. J. Bot. 59, 349-356.

LEVY, A., 1964. The accuracy of the bubble meter-method for gas flow measurement. J. of Scient. Instr. 41, 449-53.

LINDER, S., 1979. Photosynthesis and respiration in conifers. A classified reference list 1891-1977. Studia Forestalia Suecica. 149, 71pp.

LINDER, S., and TROENG, E., 1980. Photosynthesis and transpiration of a 20 year old Scots pine. In structure and function of Northern coniferous forests- An ecosystem study. Ecol. Bull. (Stockholm) 32, 165-181.

LINDER, S., and LOHAMMAR, T., 1981. Amount and quality of information required for estimating annual carbon balance of coniferous trees. In understanding and predicting tree growth. Ed. LINDER, S. Studia Forestalia Suecica. 160, 87pp.

LUDLOW, M.M., and JARVIS, P.G., 1971. Photosynthesis in Sitka spruce (Picea sitchensis (Bong.) Carr.) I. General characteristics. J. A. Ecol. 8, 925- 953.

MAHON, J.D., and DOMEY, J., 1979. A light-weight battery operated infra-red gas analyzer for field measurements of photosynthetic CO_2-exchange. Photosynthetica, 13, 459-66.

MIRANDA, H.S., 1982. A model of canopy photosynthesis and transpiration for Sitka spruce (Picea sitchensis (Bong.) Carr). PhD Thesis University of Edinburgh.

MOONEY, H.A., DUNN, E.L., HARRISON, A.T., MORROW, P., BARTHOLOMEW, B., and HAYS, R.L., 1971. Ibid. 5, 128-32.

NEILSON, R.E., LUDLOW, M.M., and JARVIS, P.G., 1972. Photosynthesis in Sitka spruce (Picea sitchensis (Bong.) Carr.) II. Response to temperature. J. A. Ecol. 9, 721- 745.

NEILSON, R.E., and JARVIS, P.G., 1975. Photosynthesis in Sitka spruce (Picea sitchensis (Bong.) Carr.) VI. Response of stomata to temperature. J. A. Ecol. 12, 879-891.

NEILSON, R.E., 1977. A technique for measuring photosynthesis in conifers by $14CO_2$ uptake. Ibid. 11, 241-50.

PARKINSON, K.J., DAY, W., and LEACH, J.E., 1980. A portable system for measuring the photosynthesis and transpiration of graminaceous leaves. J. exp. Bot. 31, 1441-53.

PRIOUL, J.L., and CHARTIER, P., 1977. Partitioning of transfer and carboxylation components of intracellular resistance to photosynthetic CO_2 fixation: A critical analysis of the methods used. Ann. Bot. 41, 789-800.

PROCTER, J.T.A., WATSON, R.L., and LANDSBERG, J.J., 1976. The carbon budget of a young apple tree. J. Amer. Soc. Hort. Sci. 101, 579-582.

ROSS, G.J.S., 1981. The use of non-linear regression methods in crop modelling. In mathematics and plant physiology. Eds. D.A. ROSE and D.A. CHARLES-EDWARDS. Academic press. 15, 269-282.

SESTAK, Z., CATSKY, J., and JARVIS, P.G., (eds), 1971. Plant photosynthetic Production: Manual of Methods. Dr.W.Junk, N.V., The Hague.

SHIMSHI, D., 1969. A rapid field method for measuring photosynthesis with labelled carbon dioxide. J. exp. Bot. 20, 381-401.

SINCLAIR, T.R., JOHNSON, M.N., DRAKE, G.M., and VAN HOUTTE, R.C., 1979. Mobile laboratory for continuous, long-term gas exchange measurements of 39 leaves. Photosynthetica, 13, 446-53.

SCHULZE, E.D., FUCHS, M.I., FUCHS, M., 1977. Spatial distribution of photosynthetic capacity and performance in a mountain spruce forest in Northern Germany. I. Biomass distribution and daily CO_2 uptake in different crown layers. Oecologia (Berl) 29, 43-61.

THORPE, M.R., SAUGIER, B., AUGER, S., BERGER, A., and METHY, M., 1978. Photosynthesis and transpiration of an isolated tree: Model and validation. Plant Cell and Environment 1, 269-277.

TROENG, E., and LINDER, S., 1981. Gas exchange in a 20-year-old stand of Scots pine. 1. Net photosynthesis of current and one-year-old shoots within and between seasons. In some aspects on annual carbon balance of Scots pine. Ed. E. TROENG. Swedish University of Agricultural Sciences, Uppsala, 1981.

TURNER, N.C., and JARVIS, P.G., 1975. Photosynthesis in Sitka spruce (Picea sitchensis (Bong.) Carr.) IV. Response to soil temperature. J. A. Ecol. 12 561-576.

WATTS, W.R., NEILSON, R.E., JARVIS, P.G., 1976. Photosynthesis in Sitka spruce (Picea sitchensis (Bong.) Carr.) VII. Measurements of stomatal conductance and $14CO_2$ uptake in a forest canopy. J. A. Ecol. 13, 623-638.

WATTS, W.R., and NEILSON, R.E., 1978. Photosynthesis in Sitka spruce (Picea sitchensis (Bong.) Carr.) VII. Measurements of stomatal conductance and $14CO_2$ uptake in controlled environments. J. A. Ecol. 15, 245-255.

WOODMAN, J.N., 1971. Variation of net photosynthesis within the crown of a large forest grown conifer. Photosynthetica 5, 50-54.

APPENDIX 1

LIST OF SYMBOLS AND ABREVIATIONS

Symbol	Definitition	Units
a	is the initial slope of the light response curve.	
A	is the leaf area.	m2
C_b	is the concentration of CO_2 in the chamber at the balance point.	$\mu mol\ mol^{-1}$
C_c	is the concentration of CO_2 in the air being added from the cylinder.	$\mu mol\ mol^{-1}$
C_i	is the intercellular space CO_2 concentration.	$\mu mol\ mol^{-1}$
f_b	is the flow of air into the assimilation chamber.	$m^{-3}\ s^{-1}$
F	is the CO_2 flux through the stomata.	$\mu mol\ m^{-2}\ s^{-1}$
F_b	is the rate of net photosynthesis at C_b.	$\mu mol\ m^{-2}\ s^{-1}$
F_m	is the asymptotic rate of photosynthesis at saturating quantum flux density.	$\mu mol\ m^{-2}\ s^{-1}$
F_n	is the rate of net photosynthesis.	$\mu mol\ m^{-2}\ s^{-1}$
F_{nm}	is the asymptotic rate of net photosynthesis at saturating quantum flux density.	$\mu mol\ m^{-2}\ s^{-1}$
g_m	is the mesophyll conductance.	$mol\ m^{-2}\ s^{-1}$
g_s	is the stomatal conductance.	$mol\ m^{-2}\ s^{-1}$
G	is the CO_2 compensation point.	$\mu mol\ mol^{-1}$
M	is the convexity coefficient.	
r^2	is the coefficient of multiple determination	
R_d	is the rate of dark respiration.	$\mu mol\ m^{-2}\ s^{-1}$
Q	is the quantum flux density.	$\mu mol\ m^{-2}\ s^{-1}$
z	is the density of CO_2 in air.	$mol\ m^{-3}$
IRGA	infra-red gas analyser.	
mse	mean square error.	
PAR	photosynthetically active radiation.	
PRT	platinum resistance thermometer.	

APPENDIX 2

LIST OF EQUIPMENT AND MANUFACTURERS

Manufacturers of items of equipment referred to in the text. The addresses refer to the U.K. unless otherwise specified.

Infrared gas analyser: Binos 2, Leybold Heraeus, 16 Endeavour Way, Durnsford Road, London, SW19 8UH.

Miniature D.C. pump: G12/02, Brey Pumps Ltd, Stockholm Road, Sutton Fields Industrial Estate, Hull, HU8 0XW.

Quick-fit connectors: Swagelok SS-QC4-D-400, Glasgow Valve and Fitting Co, 9/11 MacAdam Place, South Newmoor Industrial Estate, Irvine, KA11 4JS.

Flowmeters: Rotameter 1300-2G-3101, Fisher Controls, Rotameter Works, 330 Purley Way, Croydon, Surrey, CR9 4PG.

Miniature filters: Whatman mini filter grade 80, Whatman, Springfield Mill, Maidstone, Kent.

Null-balance diffusion porometer: Dingbat Electronics, c/o Neilson, Orcadia, Disblair Road, Newmachar, Aberdeenshire, AB4 0PL.

Cross-linked polystyrene: Q.200.5, Polypenco, Gate House, Welwyn Garden City, Hertfordshire.

Humidity sensor: Humicap 6061 HM, Vaisala, 32/36 Hazelwood Road, Northampton, NN1 1LG.

Quantum sensor: LI-190SB, Li-Cor, P.O. Box 4425, Lincoln, Nebraska 68504, 7, U.S.A.

Semiconductor temperature sensor: AD590, Farnell Electronic Components Ltd, Canal Road, Leeds, Yorkshire, LS12 2TU.

Gas mixing pumps: G27/3F, SA18/3F, SA27/3F, Wosthoff, Apparatebau, 463 Bochum, Hagenstr.30, Germany (BRD).

Precision PRT: Guildline 9535, Guildline Instruments Ltd, K7A459 Smiths Falls, Ontario, Canada.

Metal halide light source: HQI 400W, Wotan, 1 Gresham Way, Durnsford Road, London SW19 8HU.

Small D.C. fans: Micronel V241L, V466M, Radiatron Components Ltd, 76 Crown Road, Twickenham, Middlesex TW1 3ET.

Closed cell polyethylene foam: Kwikstik Inseal 7304, Dickinson Robinson Group, Chesham, Buckinghamshire HP5 1NG.

Polymethylpentene plastic: Mitsui TPX, Yarsley Technical Centre, Trowers Way, Redhill, Surrey RH1 2JN.

Portable power pack: 12.15/30, Varley Ltd, Chandos Road, Acton, London NW10 6NF.

Solarimeter: CM3, Kipp and Zonen, P.O. Box 7, Delft, Holland.

Integrating unit: MV1, Delta-T Devices, 128 Low Road, Burwell, Cambridge CB5 0EJ.

Ventilated Psychrometer: Assmann psychrometer HYT-540, Cassela, Britannia Walk, London N1 7ND.